AD-A089 485 NAVAL POSTGRADUATE SCHOOL MONTEREY CA F/G 13/10
AN EXPERIMENTAL INVESTIGATION OF THE EFFECT OF CONDENSATE INUND--ETC(U)
MAR 80 D E ESHLEMAN

UNCLASSIFIED NL

1 OF 1
AD A089485

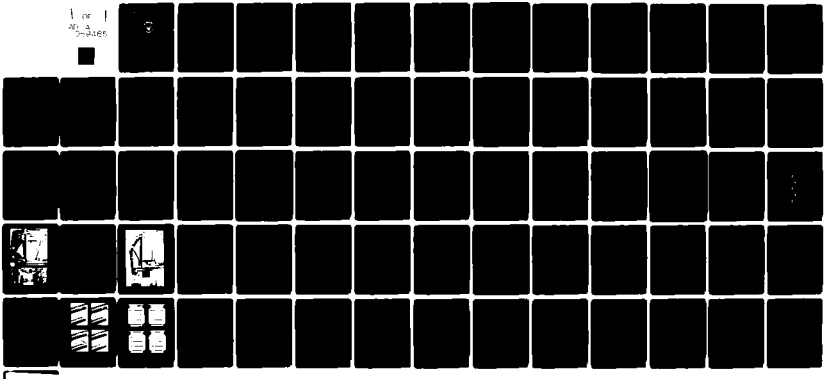

END
DATE FILMED
10-80
DTIC

NAVAL POSTGRADUATE SCHOOL
Monterey, California

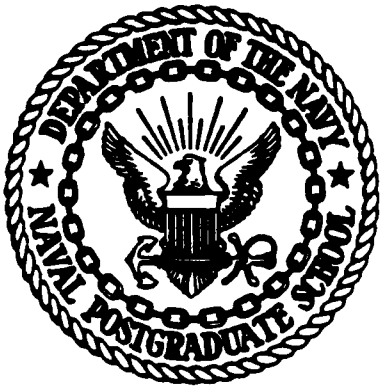

THESIS

AN EXPERIMENTAL INVESTIGATION OF THE EFFECT OF CONDENSATE INUNDATION ON HEAT TRANSFER IN A HORIZONTAL TUBE BUNDLE

by

Donald Eugene Eshleman

March 1980

Thesis Advisor: P. J. Marto

Approved for public release; distribution unlimited.

UNCLASSIFIED

SECURITY CLASSIFICATION OF THIS PAGE (When Data Entered)

REPORT DOCUMENTATION PAGE		READ INSTRUCTIONS BEFORE COMPLETING FORM
1. REPORT NUMBER	2. GOVT ACCESSION NO. AD-A089 485	3. RECIPIENT'S CATALOG NUMBER
4. TITLE (and Subtitle) An Experimental Investigation of the Effect of Condensate Inundation on Heat Transfer in a Horizontal Tube Bundle		5. TYPE OF REPORT & PERIOD COVERED Master's Thesis; March 1980
		6. PERFORMING ORG. REPORT NUMBER
7. AUTHOR(s) Donald Eugene Eshleman		8. CONTRACT OR GRANT NUMBER(s)
9. PERFORMING ORGANIZATION NAME AND ADDRESS Naval Postgraduate School Monterey, California 93940		10. PROGRAM ELEMENT, PROJECT, TASK AREA & WORK UNIT NUMBERS
11. CONTROLLING OFFICE NAME AND ADDRESS Naval Postgraduate School Monterey, California 93940		12. REPORT DATE March 1980
		13. NUMBER OF PAGES 67
14. MONITORING AGENCY NAME & ADDRESS(if different from Controlling Office)		15. SECURITY CLASS. (of this report) Unclassified
		15a. DECLASSIFICATION/DOWNGRADING SCHEDULE

16. DISTRIBUTION STATEMENT (of this Report)

Approved for public release; distribution unlimited.

17. DISTRIBUTION STATEMENT (of the abstract entered in Block 20, if different from Report)

18. SUPPLEMENTARY NOTES

19. KEY WORDS (Continue on reverse side if necessary and identify by block number)

Condensate Inundation
Heat Transfer
Horizontal Tube Bundle

20. ABSTRACT (Continue on reverse side if necessary and identify by block number)

A test facility to evaluate the effect of condensate inundation on heat transfer within a horizontal tube bundle was designed, constructed and validated. Five 15.9 mm (5/8 in.) nominal outside diameter, smooth stainless steel tubes were utilized in a vertical row. They were located in an equilateral triangular array with a spacing to diameter ratio of 1.5.

DD FORM 1 JAN 73 1473 (Page 1) EDITION OF 1 NOV 65 IS OBSOLETE S/N 0102-014-6601

UNCLASSIFIED

SECURITY CLASSIFICATION OF THIS PAGE (When Data Entered)

#20 - ABSTRACT - (CONTINUED)

Heat transfer performance was determined for each tube in the bundle. Data was taken by condensing steam at about 21 kPa (3 psia) on the outside of each tube. Each tube was cooled by water on the inside at velocities of 0.78 to 7.0 m/sec (2.56 to 23 ft/sec). The overall heat transfer coefficient was determined directly from experimental data. The inside and outside heat transfer coefficients were determined using the Wilson plot technique.

Observation of condensate flow showed lateral droplet motion along the tube in portions of the condenser as well as side drainage, particularly over the first three tubes. Outside heat transfer coefficients were lower than expected when compared to Nusselt theory, possibly due to the effects of secondary vapor flow and/or non-condensable gases. Recommendations to improve validation are provided.

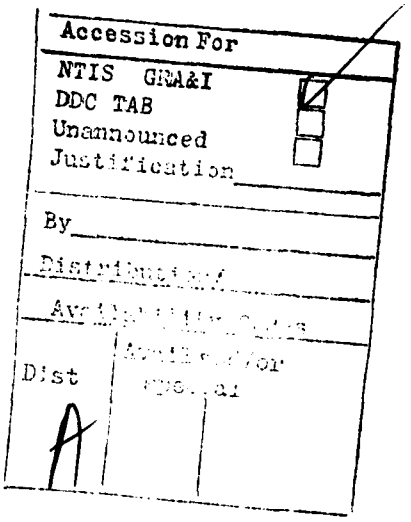

Approved for public release; distribution unlimited.

An Experimental Investigation of the
Effect of Condensate Inundation on
Heat Transfer in a Horizontal Tube Bundle

by

Donald Eugene Eshleman
Lieutenant Commander, United States Navy
B.S., United States Naval Academy, 1966

Submitted in partial fulfillment of the
requirements for the degree of

MASTER OF SCIENCE IN MECHANICAL ENGINEERING

from the

NAVAL POSTGRADUATE SCHOOL

March 1980

Author Donald E. Eshleman

Approved by: P. J. Marto
Thesis Advisor

R. H. Nunn
Second Reader

P. J. Marto
Chairman, Department of Mechanical Engineering

William M. Tolles
Dean of Science and Engineering

ABSTRACT

A test facility to evaluate the effect of condensate inundation on heat transfer within a horizontal tube bundle was designed, constructed and validated. Five 15.9 mm (5/8 in.) nominal outside diameter, smooth stainless steel tubes were utilized in a vertical row. They were located in an equilateral triangular array with a spacing to diameter ratio of 1.5.

Heat transfer performance was determined for each tube in the bundle. Data was taken by condensing steam at about 21 kPa (3 psia) on the outside of each tube. Each tube was cooled by water on the inside at velocities of 0.78 to 7.0 m/sec (2.56 to 23 ft/sec). The overall heat transfer coefficient was determined directly from experimental data. The inside and outside heat transfer coefficients were determined using the Wilson plot technique.

Observation of condensate flow showed lateral droplet motion along the tube in portions of the condenser as well as side drainage, particularly over the first three tubes. Outside heat transfer coefficients were lower than expected when compared to Nusselt theory, possibly due to the effects of secondary vapor flow and/or non-condensable gases. Recommendations to improve validation are provided.

TABLE OF CONTENTS

LIST OF TABLES

LIST OF FIGURES

NOMENCLATURE

A_n - Outside Nominal Surface Area of Tube (m^2)

A_c - Cross Sectional Area of Test Section (m^2)

C - Constant Determined from Experimental Data

C_p - Specific Heat (kJ/kg-K)

C_{wv} - Cooling Water Velocity (m/sec)

D_i - Inside Diameter (m)

D_o - Outside Diameter (m)

F_d - Drainage Factor

G - Mass Flow Rate of Cooling Water Per Unit Area (kg/m^2-sec)

GPM - Gallons Per Minute of Cooling Water Flow

h_{fg} - Latent Heat of Vaporization (J/kg)

h_i - Inside Heat Transfer Coefficient (W/m^2-K)

h_o - Outside Heat Transfer Coefficient (W/m^2-K)

h_n - Mean Heat Transfer Coefficient on n^{th} Tube (W/m^2-K)

$\bar{h}_n$ - Average Heat Transfer Coefficient over a Bundle of n Tubes

h_{Nu} - Nusselt's Heat Transfer Coefficient (W/m^2-K)

k_w - Thermal Conductivity of Water (W/m-K)

L - Length (m)

LPM - Liters Per Minute

M - Wilson Plot Slope

$\dot{m}_c$ - Mass Flow Rate of Condensate (kg/sec)

$\dot{m}_{cw}$ - Mass Flow Rate of Cooling Water (kg/sec)

n - Number of Tubes

μ - Dynamic Viscosity (kg/m-sec)

Pr - Prandtl Number

Q - Heat Transfer Rate (J/sec)

Re - Reynolds Number

ρ - Density (kg/m^3)

R_w - Wall Resistance (m^2-K/W)

T_{bc} - Bulk Temperature (C)

T_{bk} - Bulk Temperature (K)

T_{ci} - Cooling Water Inlet Temperature (C)

T_{co} - Cooling Water Outlet Temperature (C)

T_{hw} - Condensate Temperature in Primary Hotwell (C)

T_{shw} - Condensate Temperature in Secondary Hotwell (C)

T_{sv} - Temperature of Steam Vapor (C)

U_c - Corrected Overall Heat Transfer Coefficient (W/m^2-K)

U_n - Overall Heat Transfer Coefficient (W/m^2-K)

X - Abcissa of Wilson Plot

Y - Ordinate of Wilson Plot (m^2-K/W)

ACKNOWLEDGMENTS

The author wishes to express his sincerest appreciation to his thesis advisor, Dr. Paul J. Marto, for his unfailing assistance and direction. A special note of thanks is deserved by Mr. Ken Mothersell for his technical and skillful support during this project. I would also like to thank Mr. Thomas Christian and LCDR Rick Foltz for their support and assistance.

The entire faculty of the Mechanical Engineering Department is recognized for their loyal and untiring efforts in furthering my education to accomplish this goal.

Finally, and certainly at the top of the list, I thank God for the talents and abilities he has entrusted to me and for the family he has surrounded me with, without whose loving support, sacrifices, and understanding this project could never have been completed.

I. INTRODUCTION

A. BACKGROUND INFORMATION

It has been well documented by Search [1] that naval marine condensers have been extremely conservative in design. Search concluded that heat transfer enhancement methods could decrease condenser space to weight ratio thereby establishing new design criteria for marine condensers.

It has been the objective of past research by Beck [2], Pence [3], Reilly [4], Fenner [5], Manvel [6] and Ciftci [7] to investigate the enhancement of heat transfer on single horizontal tubes. Their research concentrated on using different tube materials and various tube geometries. Each of these investigations recommended that the effect of both inundation or condensate rain, and vapor velocity be examined for these enhanced tubes.

Any attempt to understand the effect of inundation and vapor velocity must begin with the classical equation derived by Nusselt [8] for predicting the mean condensate heat transfer coefficient for a column of n horizontal tubes. It is normally written as a ratio of the average heat transfer coefficient for a column of n horizontal tubes ($\bar{h}_n$) to that of the uppermost tube (h_{Nu}). The following relationship was obtained:

$$\frac{\bar{h}_n}{h_{Nu}} = n^{-1/4} \qquad (1)$$

where

n = no. of tubes in a column.

Experimental results to date indicate that Equation (1) underestimates the heat transfer. The above relationship was derived assuming: (1) condensation of a saturated vapor at negligible velocity and (2) laminar flow of the condensate film in a continuous sheet from one tube to the next at a constant temperature difference (as measured between the vapor and the wall) for all tubes in the bank.

Neither of the above assumptions correspond to actual steam condenser conditions. Considering the first assumption, it is well known that with variable steam turbine speeds, the velocity of steam is often not negligible. Considering the second assumption, investigation, including filming, by Skklover and Buevich [9] reveals that condensate dropping onto the tube situated below in an "in-line" configuration does not drain as a continuous laminar sheet. In fact, it hardly spreads along the length of the tube at all, but rather rolls over it's perimeter forming droplets which locally thicken the film. Dr. David Eissenberg of the Oak Ridge National Laboratory in an unpublished work preceding his Ph.D. dissertation [10] noted that the droplets do not only strike the tops of the tubes below, but strike anywhere on the upper half.

Eissenberg [10] performed experimental tests on a vertical column of five tubes in a triangular arrayed horizontal bank

with horizontal steam flow. His results were well above those predicted by Nusselt. He proposed a "side drainage" model with a droplet path as shown in Figure 1. His model assumes that some drainage occurs from the tube bottom to tube side in triangular arrayed tube banks thereby resulting in only part of the lower tube being inundated and the heat transfer coefficient for the tube being increased. If all the drainage was by the "side drainage" model, he showed that:

$$\frac{\bar{h}_n}{h_{Nu}} = 0.6 + 0.42n^{-1/4} \qquad (2)$$

His experimental results fell between his side drainage prediction and that of Nusselt.

A literature review reveals data scatter between that of Eissenberg and Nusselt. The data scatter results from the many experimental designs decided on by the individual authors. In summary, it can be generalized to say that in most cases the data has been fit to various modified forms of Equation (1) in which the exponent is empirically determined:

$$\frac{\bar{h}_n}{h_{Nu}} = n^{-s} \qquad (3)$$

where values of s have been reported from 0.07 to 0.223.

The effects of inundation and steam velocity are normally described in the literature as separate from each other. In fact, they occur simultaneously and their combined effect on

condensation in a tube bundle is complex. Fujii [11] used the experiments of Nobbs and Mayhew to correlate the effect of inundation and vapor shear. The data for "in-line" tube banks resulted in Equation (4) for the first or uninundated tube :

$$Nu_m^\circ = 10.74\ Re_L^{0.312} \qquad (4)$$

where

Nu_m° = Nusselt number, $h_o d_o / k_L$ for pure steam without inundation;

Re_L = two-phase Reynolds number, $U_\infty d_o / \nu_L$;

k_L = thermal conductivity of liquid,

d_o = outside diameter of tube;

ν_L = kinematic viscosity of liquid, and

U_∞ is vapor velocity.

Nu_m / Nu_m° is computed for the data and inundated tubes resulting in Equation (5):

$$Nu_m / Nu_m^\circ = \left(\frac{Re_L}{2 \times 10^6}\right)^{0.071 (w/w^\circ)^{0.65}} \qquad (5)$$

where

Nu_m = mean Nusselt number for a tube

w = rate of inundation falling onto a tube

w° = rate of condensation of a tube corresponding to Nu°.

Fujii [11] determined that for the staggered tube bank, the inundation effect was smaller than that for the in-line bank. This would follow from examination of Eissenberg's side drainage model.

Experimental data resulting from varying inundation rates and steam velocities is sufficiently scattered to suggest that no existing correlation adequately represents all the available data. This is because there are so many variables that affect condenser performance, some of which have yet to be explored (e.g., direction of steam flow, pitch to diameter ratio of the tubes, non-condensable gas effects, and the effects due to pitch and roll in a marine environment). Research is presently being conducted in the United Kingdom aimed at producing a model of condensation suitable for sophisticated condenser performance calculations. However, the results have yet to be published.

B. OBJECTIVES OF THIS WORK

In order to evaluate the effect of inundation on a bank of enhanced tubes, it was necessary to establish data on a bank of smooth tubes as a standard of comparison. The objectives of this work were therefore:

1. To modify the existing experimental apparatus to accommodate a bank of five tubes.

2. To experimentally validate the system by comparing the experimental results to theoretical predictions, thereby establishing a data base on which to further study the various parameters affecting heat transfer within an enhanced tube bundle.

II. EXPERIMENTAL APPARATUS

A. INTRODUCTION

The existing test facility was designed by Beck [2] and built and tested by Pence [3]. In order to accomplish the goals of this work, major modifications were made to the original apparatus. In the following description of the experimental apparatus, attention will be focused on the changes and additions to the existing layout.

B. STEAM SYSTEM

The steam system is shown in Figure 3. The supply of steam is locally generated and supplied to the building which houses the experimental apparatus. The steam is provided via a 19.05mm diameter line and a steam inlet valve (MS-2). A pressure gage is located just prior to the steam separator which monitors the supply pressure as it is adjusted by (MS-2). Following the steam separator, a line strainer provides additional protection from contamination. After the strainer, the steam proceeds through a 31.75mm diameter line which provides for two possible steam paths. The primary path for system operation is via the throttling valve (MS-3), through a desuperheater and into the test condenser. Inside the condenser, the steam is condensed on the test tubes. The steam which is not condensed proceeds via the vapor outlet on the test condenser to the secondary condenser. The secondary steam flow path is used to accomplish system stabilization

during start up and to control the mass flow rate of steam to the condenser during operation. Steam proceeds via (MS-4) directly to the secondary condenser. All steam lines except the primary path downstream of (MS-3) were insulated with 25.4mm thick fiberglass insulation.

C. TEST CONDENSER

The test condenser is shown from various views in Figures 4, 5 and 6. Steam enters via the top and proceeds over the baffle separators and through a flow straightener, which is covered with three layers of 150 mesh screen, to the tube bundle. The condensate collects at the bottom of the condenser and flows out one of the two 12.7mm diameter openings at either end of the condenser to the hotwell where it can be collected and measured.

A considerable modification was made to the viewing section to accommodate observation of the condensation process. Three separate viewing windows each 203mm by 140mm by 12.7mm and made of pyrex plate glass were installed to provide maximum viewing of the active tubes while maintaining structural integrity.

The tube sheet arrangement is shown in Figure 6. The tubes are arranged in a typical naval condenser spacing to diameter ratio of 1.5. There were five 15.9mm OD, 1.14mm thick, 304 stainless steel tubes that had cooling water passing through them. Although typical naval condenser tubes are made of 90-10 copper-nickel, the choice of 304 stainless

steel was based on "on-hand" stock and the fact that the principles of inundation do not rely on tube material although perhaps the heat flux may change due to a different tube wall resistance. The remaining half tubes were made of 15.9mm OD aluminum bar stock and were fastened by screws to the outside wall of the steam flow path. This arrangement was selected to best simulate the steam flow conditions in a section of tubes within an actual condenser. The five test tubes are singularly removable. The top tube can be replaced by a 304 stainless steel porous tube which could simulate various condensate inundation rates.

The test condenser was insulated with a 25.4mm thick sheet of Armorflex insulation.

D. CONDENSATE SYSTEM

The condensate system had no revisions and is identical to that shown in Figure 7 which is taken from Ref. [7]. The test condenser hotwell collects the condensate from the test tubes, while the secondary condenser hotwell collects the condensate from the secondary condenser. Valve (C-1) allows the isolation of the test condenser hotwell for condensate measurement. Since house steam was used as the steam supply system, the condensate collected in the hotwells is pumped back to the house system by the condensate pump via valve (C-3). The condensate lines were insulated with 19.1mm thick Johns-Manville Aerotube insulation.

E. COOLING WATER SYSTEM

The cooling water system is shown in Figure 8. The water used was normal house water which had been passed through a water softener on the way to the supply tank. The water is pumped from the supply tank by a 5HP electric driven pump. It is routed to the flowmeter header via 51mm OD plastic pipe. The flow of cooling water for each test tube is then individually controlled by it's own rotameter. Each rotameter allowed a maximum flowrate of 70.4 LPM. The cooling water after passing through the test section was piped back to the supply tank. A separate system pumped the water through a filter and cooling tower returning the cooled water to the supply tank in an effort to maintain a constant cooling water inlet temperature.

After leaving the rotameters, the system piping was reduced to 15.9mm, ensuring a distance of 1 meter ahead of the test section to ensure a fully developed velocity profile while passing through the test section.

F. SECONDARY SYSTEMS

1. Vacuum System

The vacuum in the test condenser and secondary condenser was maintained by a mechanical vacuum pump and a vacuum regulator which induces air into the system. The vacuum pump takes a suction from the secondary condenser hotwell which is connected to the test condenser hotwell via discharge piping. A cold trap at the inlet of the vacuum

pump forces incoming vapor to pass over a system of refrigerated copper coils. This removes steam and entrained water from the vacuum line preventing moisture contamination of the vacuum pump oil. The vacuum pump outlet is vented through a roof exhaust fan to avoid a health hazard from breathing any oil vapor exhausted by the pump. A schematic diagram of this system can be found in Figure 9 which is taken from Ref. [7].

2. Desuperheater System

The desuperheater removes sensible heat from the superheated system by injecting water at about 60 C via the existing feedwater system through valve (DS-1) and a rotameter. The desuperheater is a 267mm diameter stainless steel can, 457mm high, having four nozzles inserted equidistant around the circumference of the inner top of the can. The nozzles are a fan type and are positioned such that the spray is downward at a 45° angle to allow for better mixing. A collection tank is located on the bottom of the desuperheater to allow for drainage of condensate. This system can be isolated by valve (DS-2).

G. INSTRUMENTATION

1. Flow Rate

a. Cooling water flow rate was measured individually for the five separate tubes. Each flow rate was determined by a rotameter with a capacity of 70.4 LPM (18.6 GPM). The calibration procedure used was identical to that listed in Appendix A of Ref. [3].

b. Steam velocity was determined by calculation;

$$\text{Vel.} = \frac{\dot{m}_{cond}\, v}{A_c} \qquad (7)$$

where

$\dot{m}_{cond}$ = Mass flow rate of condensate (kg/sec), = Q/h_{fg}

A_c = Cross sectional area (m^2), and

v = Specific volume of vapor (m^3/kg).

2. Pressure

Two different pressure sensing devices were used during experimentation. They were a Bourdon tube pressure gauge which measured steam pressure and an absolute pressure transducer coupled with a 760mm mercury manometer which was used to measure test condenser pressure.

3. Temperature

Stainless steel sheathed, copper-constantan thermocouples were used as the primary temperature monitoring devices. Figure 5 shows the location of the five vapor thermocouples. The remaining 30 thermocouples of this type were located as shown in Figure 8, six on each tube, two measuring cooling water inlet temperature and four measuring cooling water outlet temperature. Calibration procedures of the thermocouples were identical to those listed in Appendix A of Ref. [3].

4. Data Collection and Display

An Autodata collection system was utilized to record and display the temperatures in degrees Celsius obtained from the primary stainless steel thermcouples and to record and display the pressure in cm of Hg inside the test condenser. Table I lists the channel numbers and location of these devices.

III. EXPERIMENTAL PROCEDURES

A. OPERATING PROCEDURES

1. Preparation of Condenser Tubes

Prior to installation, each tube was properly prepared to ensure filmwise condensation. The cleaning procedure is listed in Appendix A of Ref. [7].

2. System Operation and Steady State Conditions

The basic operating instructions developed by Pence [3] and modified by Reilly [4] were used. The only change to the procedures as listed in Appendix B of Ref. [7] was that instead of one cooling water flowmeter to adjust, the experimenter had five to set as desired.

In general it takes from two to three hours from initial light off until steady-state conditions are established. The parameters used in determining steady-state conditions were cooling water inlet temperature and steam inlet temperature. If the cooling water inlet temperature did not vary more than ± 0.6 C/HR or the steam temperature did not vary more than ± 0.3 C/MIN, state steady was considered achieved.

The time for the system to stabilize between changes in cooling water flow rate during the Wilson Plot technique was approximately ten minutes. This time increment is suspect as other investigators waited about one hour for stabilization between changes. It must be pointed out however that

the amount of time required to collect data over five tubes in a system that cannot be shut down and repeated the next day prohibits the greater time increment between data points for the Wilson Plot.

The general set up for the data taken in this research was a steam velocity of approximately 5m/sec steam temperature of 64 C and a test condenser pressure of approximately 21 KPa.

B. DATA REDUCTION PROCEDURES

The raw data collected for each tube can be found in the Tables Section beginning on page 32. The following standard heat transfer equations were used to reduce the raw data into a form that can be used for evaluation.

1. Overall Heat Transfer Coefficient (U_n)

$$U_n = \frac{\dot{m}c_p}{A_n} \ln \left(\frac{T_{sv} - T_{ci}}{T_{sv} - T_{co}}\right) \qquad (8)$$

2. Corrected Overall Heat Transfer Coefficient (U_c)

$$U_c = \frac{1}{\frac{1}{U_n} - R_w} \qquad (9)$$

where R_w is the wall resistance corresponding to different tube materials. This equation allows for the comparison of tubes of different materials for the same steam and cooling water condition within the test condenser.

3. Inside Heat Transfer Coefficient (h_i)

$$Nu = \frac{h_i D_i}{k} = 0.036\ Re^{0.8}\ Pr^{1/3}\ (L/D)^{-0.054} \tag{10}$$

Equation (10) was selected because both the Dittus-Boelter and Sieder-Tate relationships which are commonly used assume a fully developed velocity, as well as, thermal profile. In this research, it was suspected that, although the velocity profile was believed to be fully developed, the thermal profile was not fully developed. When an L/D ratio of 57.6 is used in Equation (10) a constant of 0.029 results. This was validated by computing the average of the first three tube constants obtained as a result of the Wilson Plot technique. Wilson Plots for each tube are found as Figures 10 through 14.

4. Outside Heat Transfer Coefficient (h_o)

$$h_o = \frac{1}{\frac{1}{U_n} - R_w - \frac{D_o}{D_i\ h_i}} \tag{11}$$

The outside heat transfer coefficient is the parameter that is used to compare results of each tube in the bundle. Two very important assumptions were made in using this equation.

a. The resistance due to fouling was equal to zero. This assumption is supported by the fact that the tubes were new, chemically cleaned and smooth. Also, treated soft water was used as the cooling medium.

b. The resistance due to non-condensable gases was equal to zero. This assumption was supported by the fact that the system was tested for air-tightness and found to be secure. In addition, it was believed that the velocity of steam passing through the test section was sufficiently large to keep the system purged of any non-condensables that might collect in the test section.

C. DATA REDUCTION COMPUTER PROGRAM

Reilly [4] developed the existing program in Fortran language. During this work, his program was translated into Basic language for use with the HP 9845 computer. This was done because of the author's desire to improve the speed and reliability of data reduction. Ultimately, this program with minor modifications, can be used in an integrated system between the Autodata Nine data collector and the HP 9845 computer. This will allow automatic data input with realtime data output for the experimenter.

IV. RESULTS AND DISCUSSION

The validation of the experimental system was done first by comparing the first tube of this configuration with the smooth, 15.9mm OD tube of Fenner [5]. Secondly, the average heat transfer coefficient over n tubes divided by the heat transfer coefficient of the first tube for this experiment was plotted for comparison to the theoretical curves based on Equations (1) and (2).

The comparison of the number one tube of this research with that of a similar tube tested by Fenner [5] is shown in Figure 15. The discrepancies are attributed to the fact that the present system was operated at a steam velocity approximately three times the value used by Fenner, thereby causing the outside heat transfer coefficient to be higher during these tests. The general agreement was sufficient to validate the data input and reduction program. The plots for tube #2 and #3 show the expected decrease in overall heat transfer as one proceeds down through the bundle of tubes. This is caused by the decrease in vapor velocity as steam is condensed as it flows downward and the fact that the condensate film is thicker on the lower tubes due to inundation from above.

Figures 10 through 14 are the Wilson Plots that assist in determining the constant in Equation (10). The first three tubes yield good linear plots with slopes which provide

constants of .026, .030 and .033 respectively. The slopes of the Wilson Plots for tubes #4 and #5 provided constants of .048 and .020 which were considered invalid. The data reduction program gives the user the option of using the constant solved for via the Wilson Plot technique or inputing one of his own choosing. In this work, since the constant 0.029 was the average over the first three tubes, it was used as input for all the tubes to determine the inside heat transfer coefficient which in turn was then used in the determination of the outside heat transfer coefficient.

The ratio of $\bar{h}_n/h_1$ as listed in Table XII was determined by taking the average outside heat transfer coefficient h_o for n tubes and averaging them, then dividing by the outside heat transfer coefficient of the first tube (h_1). The results of Table XII are then plotted on Figure 16 along with the theoretical equations of Nusselt and Eissenberg. Based on the observations of condensate flow, shown in Figure 17 it was expected that the data over the first three tubes, where "side drainage" was the dominant mode of flow, would approach the Eissenberg curve. The data for tubes #4 and #5 was expected to fall closer to the Nusselt curve due to the observed presence of gravity dominated flow, but certainly not below it.

The cause for lower outside heat transfer coefficients than expected may be due to several phenomena. During observation of the condensate flow patterns on the first three

tubes, there was evidence of droplet migration, from the ends of the tubes towards the center. This migration is shown pictorially in Figure 18 and is presumably due to vapor flow axially along the tube. This vapor flow causes a non-uniform heat transfer rate across the length of the tube because of the increase in film thickness that develops toward the center of the tube instead of a thinner condensate film which would result if the vapor flow was uniformly downward. This thickening of the film in the central part of the tube would result in a lower average heat transfer coefficient than expected.

The severe drop in performance of tubes number four and five indicate that either there is a very low mass flow of steam remaining to be condensed or there is a concentration of non-condensables that is affecting heat transfer performance. The latter is most suspect as the data for tubes four and five occurred between eight and twelve hours into the run allowing a significant buildup of non-condensables if steam velocity was not sufficient to purge it out. It is conceivable that the non-condensables entered into the system from the steam side possibly from the house steam, the desuperheater spray system or via the vacuum bleed valve which was slightly open during operation to maintain desired test condenser pressure. The presence of secondary flow would also lead to a stagnation area which would trap non-condensables in pockets near the bottom and sides of the test section.

V. CONCLUSIONS AND RECOMMENDATIONS

The experimental data obtained leads to the following conclusions:

1. The system as modified is a valid test facility for further experimentation investigating the effect of innundation and vapor velocity.

2. There is evidence of secondary flow of steam within the test condenser which is suspected to have influenced the results.

3. The measured ratio of $\bar{h}_n/h_1$ is lower than expected.

The following recommendations are provided:

1. Improve the steam flow path to ensure a uniform downward profile through the bundle. This can be accomplished by either a re-design of the steam inlet section or by a series of baffles spaced between the tubes to reduce the secondary flow effects.

2. Measure the non-condensable gas concentration using the method described in Ref. [12].

3. Operate the system at higher steam velocities and mass flow rates to ensure adequate purging and heat transfer at the lower tubes. In addition, longer stabilization times between cooling water velocity changes should be tried in order to obtain more consistent Wilson Plots.

VI. TABLES

Table I

Location of Stainless Stell Sheathed
Copper Constantan Thermocouples

CHANNEL NUMBER	LOCATION	CHANNEL NUMBER	LOCATION
45	T_{sv}	82	T_{co} #2
46	T_{sv}	83	T_{co} #2
47	T_{sv}	84	T_{co} #2
48	T_{sv}	85	T_{co} #2
49	T_{sv}	86	T_{co} #3
52	T_{hw}	87	T_{co} #3
54	T_{shw}	88	T_{co} #3
70	T_{ci} #1	89	T_{co} #3
71	T_{ci} #1	90	T_{co} #5
72	T_{ci} #2	91	T_{co} #5
73	T_{ci} #2	92	T_{co} #4
74	T_{ci} #3	93	T_{co} #4
75	T_{ci} #3	94	T_{co} #4
76	T_{co} #1	95	T_{co} #4
77	T_{co} #1	96	T_{co} #5
78	T_{co} #1	97	T_{co} #5
79	T_{co} #1	98	T_{co} #5
80	T_{ci} #4	99	T_{co} #5
81	T_{ci} #4		

Table II

Raw Data for Tube Number 1

% FLOW	T_{ci} (°C)	T_{co} (°C)	T_{sv} (°C)	GPM
10	22.5	30.9	64.2	1.92
12.5	22.9	30.5	64.0	2.4
15	23.5	30.5	64.2	2.88
17.5	23.7	30.0	63.9	3.36
20	24.0	29.9	64.5	3.84
25	24.1	29.4	64.0	4.80
40	24.2	28.2	64.4	7.68
50	24.3	27.7	64.4	9.67
90	24.5	26.8	64.8	17.29

Table III

Results for Tube Number 1

h_i	h_o	C	Re	C_{wv}
4404.	11696.	.029	12999.	.78
5265.	12631.	.029	16249.	.97
6113.	13272.	.029	19622.	1.17
6904	12610.	.029	22820.	1.36
7691.	12419.	.029	26135.	1.55
9173.	14007.	.029	32533.	1.94
13276.	13958.	.029	51458.	3.11
15926.	13774.	.029	64520.	3.91
15926.	13774.	.029	64520.	3.91
25248.	14872.	.029	114516.	7.00

U_n	U_c	Q	$\dot{m}_c$
2510.	2931.	4277.	.001821
2855.	3413.	4837.	.002059
3157.	3853.	5345.	.002276
3338.	4125.	5613.	.002390
3519.	4407.	6008.	.002557
3978.	5151.	6746.	.002872
4680.	6391.	8149.	.003469
4987.	6978.	8723.	.003713
4987.	6978.	8723.	.003713
5915.	8942.	10552.	.004492

Table IV

Raw Data for Tube Number 2

% FLOW	T_{ci} (°C)	T_{co} (°C)	T_{sv} (°C)	GPM
10	24.1	31.8	64.1	1.92
12.5	24.1	31.0	64.3	2.40
15.0	24.1	31.0	64.3	2.40
17.5	24.1	29.9	64.2	3.36
20.0	24.2	29.5	64.3	3.84
25.0	24.1	28.9	64.6	4.80
40.0	24.5	28.0	64.5	7.68
50.0	24.7	27.6	64.2	9.67
70.0	24.7	27.6	64.2	9.67
90.0	25.2	27.0	64.6	17.29

Table V

Results for Tube Number 2

h_i	h_o	C	Re	C_{wv}
4468.	9097.	.029	13341.	.78
5317.	8956.	.029	16539.	.97
5317.	8956.	.029	16539.	.97
6916.	9234.	.029	22892.	1.36
7682.	8892.	.029	26081.	1.55
9147.	9609.	.029	32364.	1.94
13283.	9759.	.029	51512.	3.11
15954.	9461.	.029	64724.	3.91
15954	9461.	.029	64724.	3.91
25381.	8971.	.029	115605	7.00

U_n	U_c	Q	$\dot{m}_c$
2386.	2763.	3918.	.001668
2627.	3092.	4390.	.001869
2627.	3092.	4390.	.001869
3046.	3688.	5167.	.002200
3162.	3860.	5397.	.002297
3516.	4402.	6111.	.002601
4091.	5341.	7130.	.003035
4283.	5673.	7439.	.003167
4283.	5673.	7439.	.003167
4694.	6417.	8256.	.003515

Table VI

Raw Data for Tube Number 3

% FLOW	T_{ci} (°C)	T_{co} (°C)	T_{sv} (°C)	GPM
10	24.9	32.5	64.82	1.92
12.5	25.0	31.8	64.76	2.40
15.0	25.1	31.1	64.60	2.88
17.5	25.3	30.8	64.58	3.36
20.0	25.3	30.3	64.74	3.84
25.0	25.3	29.6	64.48	4.80
40.0	25.2	28.2	64.62	7.68
50.0	25.2	27.8	64.48	9.67
70.0	25.2	27.8	64.48	9.67
90.0	25.3	26.9	64.46	17.29

Table VII

Results for Tube Number 3

h_i	h_o	C	Re	C_{wv}
4506.	8516.	.029	13548.	.78
5369.	8667.	.029	16831.	.97
6191.	8094.	.029	20073.	1.17
6999.	8237.	.029	23395.	1.36
7766.	7794.	.029	26599.	1.55
9247.	7735.	.029	33010.	1.94
13353.	7077.	.029	51999.	3.11
16018.	7569.	.029	65200.	3.91
16018.	7569.	.029	65200.	3.91
25381.	7313.	.029	115605.	7.00

U_n	U_c	Q	$\dot{m}_c$
2355.	2722.	3866.	.001646
2615.	3076.	4324.	.001841
2757.	3274.	4579.	.001949
2945.	3542.	4897.	.002085
3025.	3659.	5089.	.002166
3244.	3983.	5471.	.002329
3535.	4432.	6110.	.002601
3852.	4941.	6668.	.002839
3852.	4941.	6668.	.002839
4196.	5522.	7339.	.003124

Table VIII

Raw Data for Tube Number 4

% FLOW	T_{ci} (°C)	T_{co} (°C)	T_{sv} (°C)	GPM
10	25.1	29.1	64.56	2.88
12.5	25.1	28.6	64.78	3.36
15.0	25.0	28.2	64.58	3.84
17.5	25.2	28.2	64.68	4.32
20.0	24.9	27.7	64.50	4.80
25.0	24.7	27.1	64.68	5.76
40.0	24.6	26.4	64.56	7.68
60.0	24.6	26.4	64.56	7.68
70.0	24.8	25.7	64.72	17.29
90.0	24.8	25.7	64.72	17.29

Table IX

Results for Tube Number 4

h_i	h_o	C	Re	C_{wv}
6120.	3149.	.029	19662.	1.17
6904.	2994.	.029	22820.	1.36
7660.	3059.	.029	25945.	1.55
8427.	3197.	.029	29249.	1.75
9125.	3249.	.029	32228.	1.94
10510.	3148.	.029	38351.	2.33
13168.	2917.	.029	50706.	3.11
13168.	2917.	.029	50706.	3.11
25131.	2996.	.029	113553.	7.00
25131.	2996.	.029	113553.	7.00

U_n	U_c	Q	$\dot{m}_c$
1789.	1994.	3054.	.001300
1804.	2012.	3118.	.001328
1882.	2110.	3259.	.001387
1985.	2240.	3437.	.001463
2047.	2319.	3565.	.001518
2074.	2354.	3667.	.001561
2060.	2335.	3668.	.001562
2060.	2335.	3668.	.001562
2294.	2641.	4130.	.001758
2294.	2641.	4130.	.001758

Table X

Raw Data for Tube Number 5

% FLOW	T_{ci} (°C)	T_{co} (°C)	T_{sv} (°C)	GPM
10	24.6	28.3	64.36	1.92
12.5	24.5	27.7	64.64	2.40
15.0	24.4	27.3	64.54	2.88
17.5	24.3	26.9	64.36	3.36
20.0	24.2	26.4	64.24	3.84
25.0	24.1	25.9	64.22	4.80
40.0	24.0	25.3	64.22	7.68
50.0	24.0	25.1	64.16	9.67
70.0	24.0	25.1	64.16	9.67
90.0	24.1	24.8	64.14	17.29

Table XI

Results for Tube Number 5

h_i	h_o	C	Re	C_{wv}
4392.	1658.	.029	12932.	.78
5229.	1696.	.029	16047.	.97
6032.	1811.	.029	19155.	1.17
6804.	1853.	.029	22230.	1.36
7545.	1708.	.029	25246.	1.55
8988.	1674.	.029	31358.	1.94
13037.	1861.	.029	49801.	3.11
15658.	1959.	.029	62572.	3.91
15658.	1959.	.029	62572.	3.91
24896.	2170.	.029	111640.	7.00

U_n	U_c	Q	$\dot{m}_c$
1090.	1163.	1184.	.000802
1160.	1242.	2037.	.000867
1256.	1354.	2216.	.000943
1312.	1418.	2318.	.000987
1263.	1361.	2242.	.000954
1282.	1384.	2293.	.000976
1469.	1604.	2650.	.001128
1563.	1717.	2824.	.001202
1563.	1717.	2824.	.001202
1775.	1976.	3213.	.001368

Table XII

Data Results for Figure 14

$\bar{h}_n/h_1$	n
1	1
.849	2
.765	3
.632	4
.533	5

VII. FIGURES

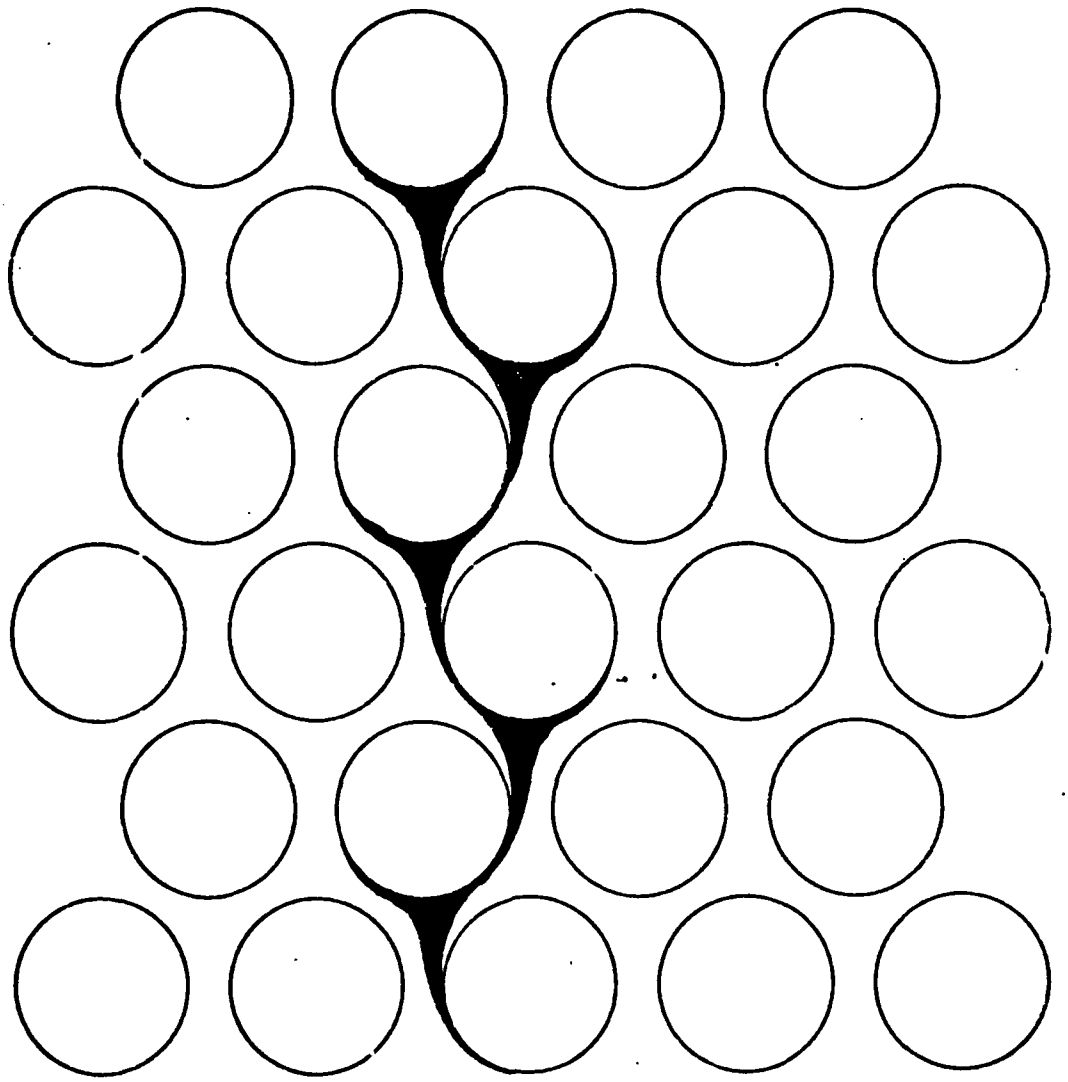

Fig. 1. Droplet Path Through a Tube Bundle with Side Drainage

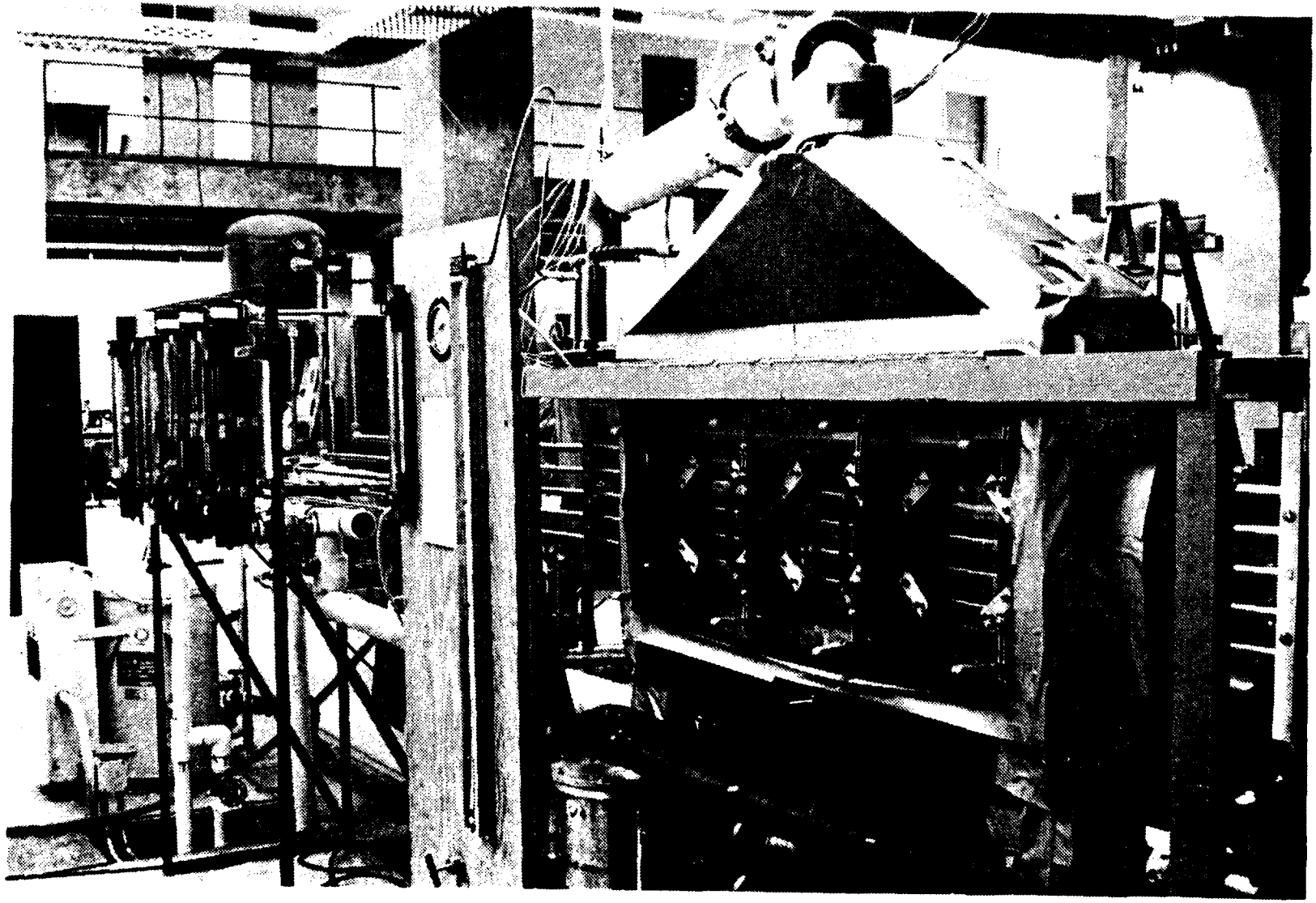

Fig. 2. Photograph of Test Facility

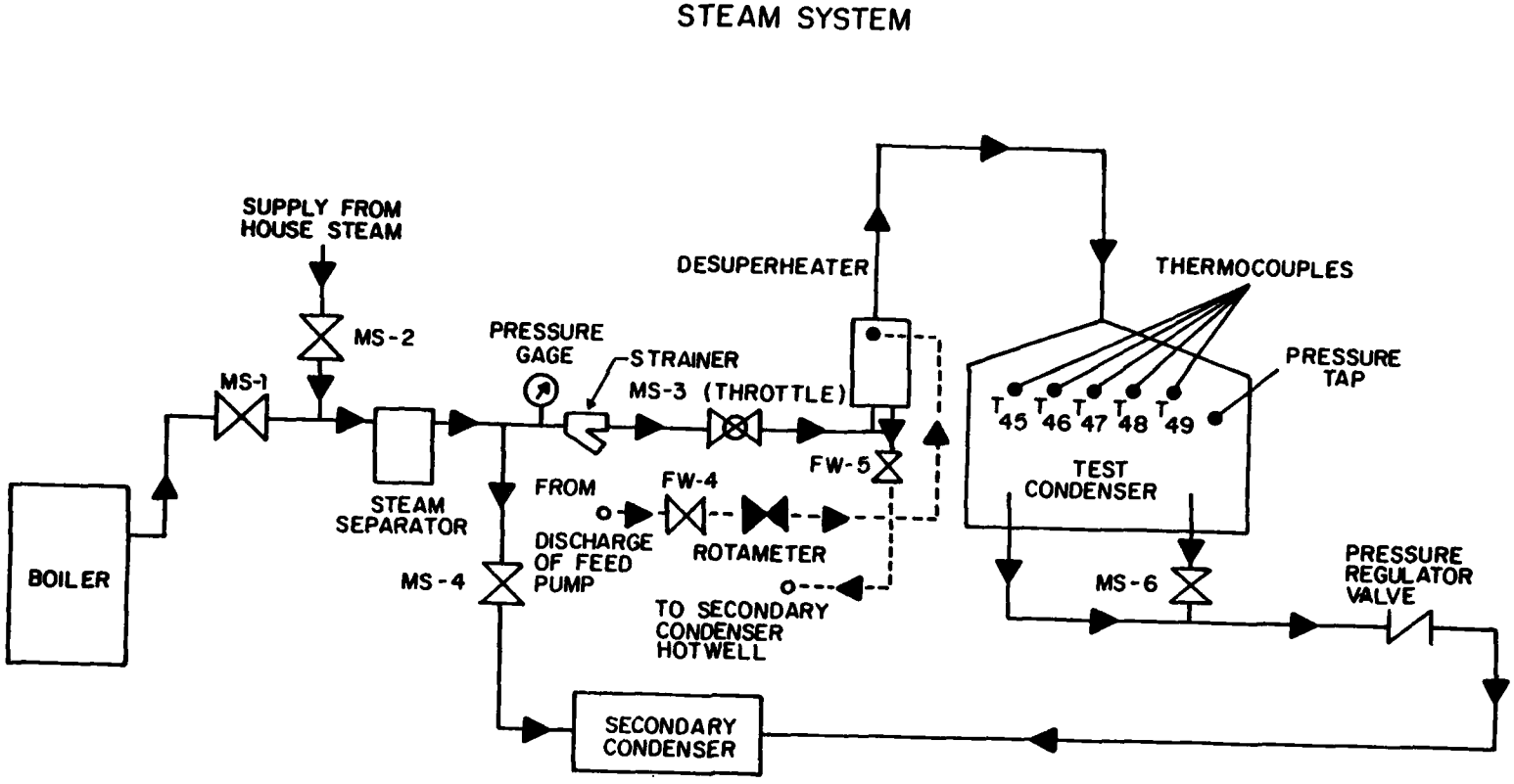

Fig. 3 Schematic Diagram of Steam System.

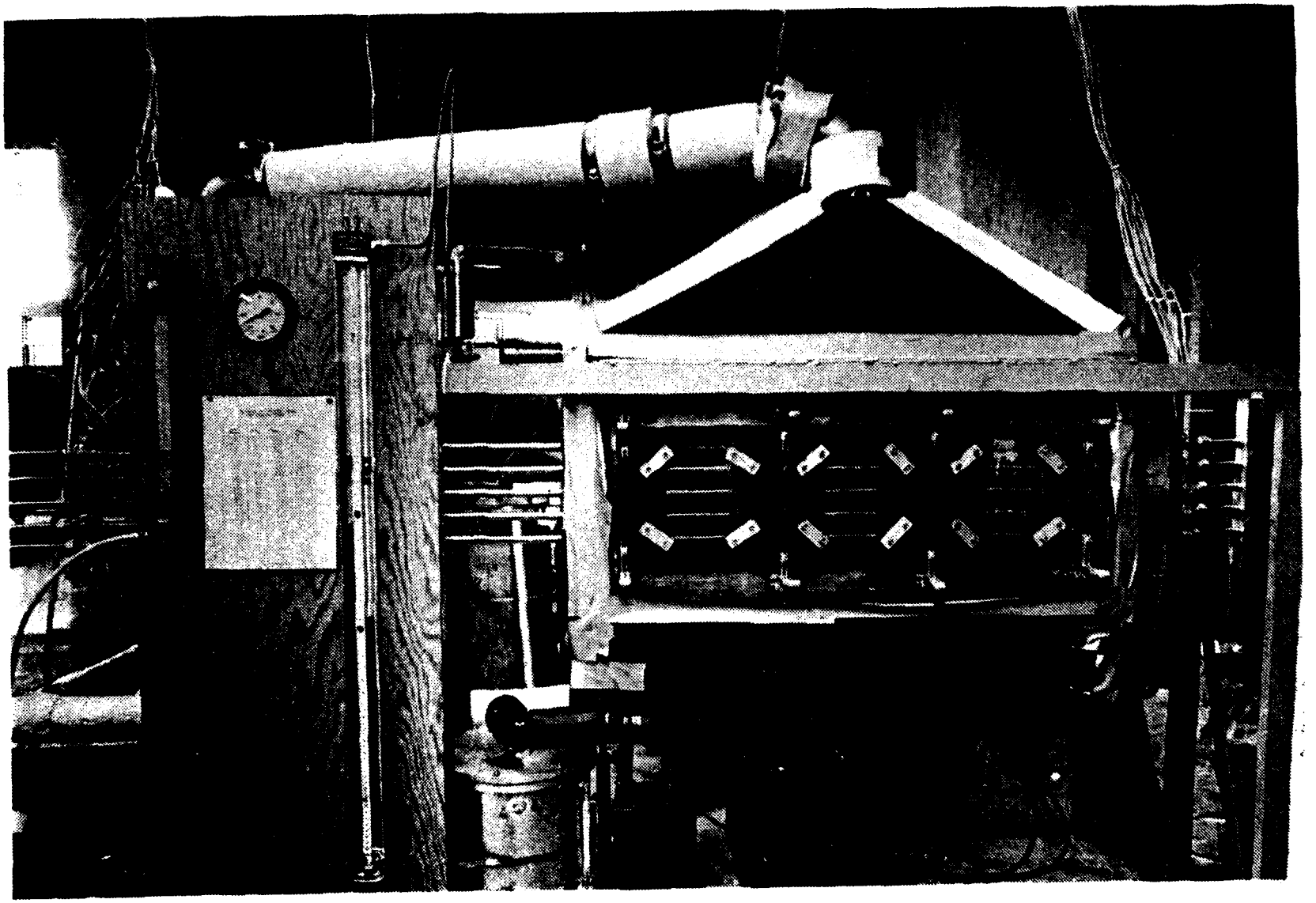

Fig. 4. Photograph of Test Condenser with Partial Insulation

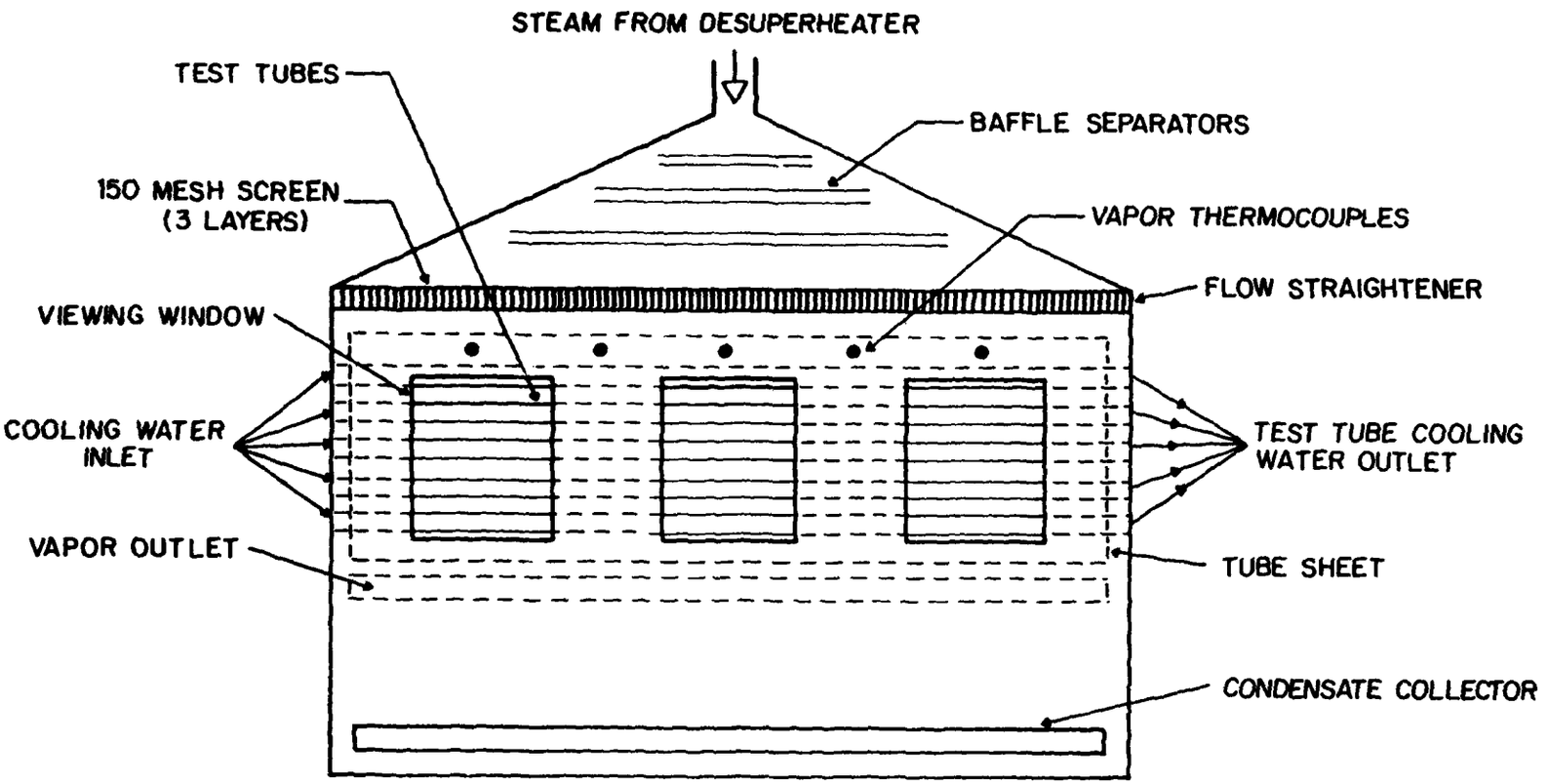

Fig. 5 Test Condenser Schematic, Front View.

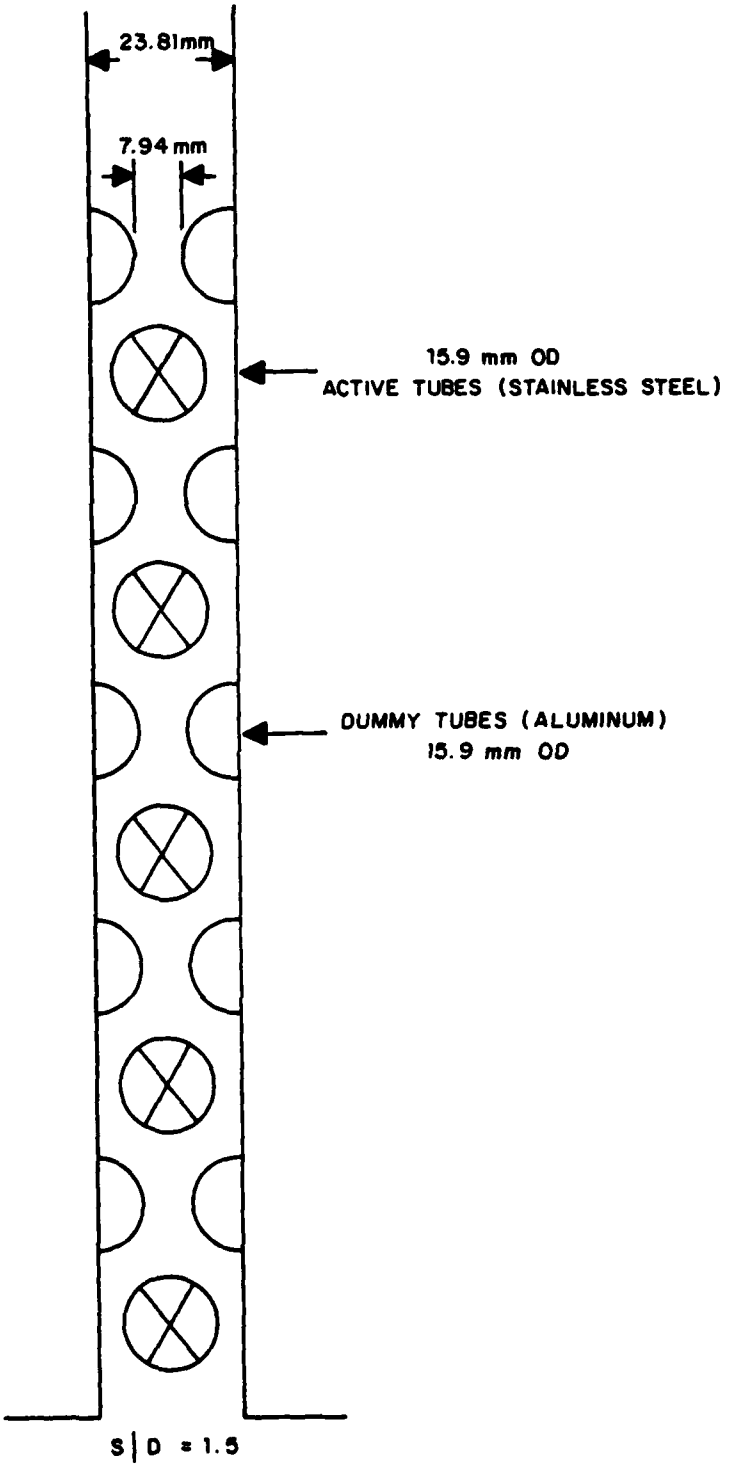

Fig. 6 Schematic Side View of Test Tube Arrangement.

CONDENSATE AND FEEDWATER SYSTEMS

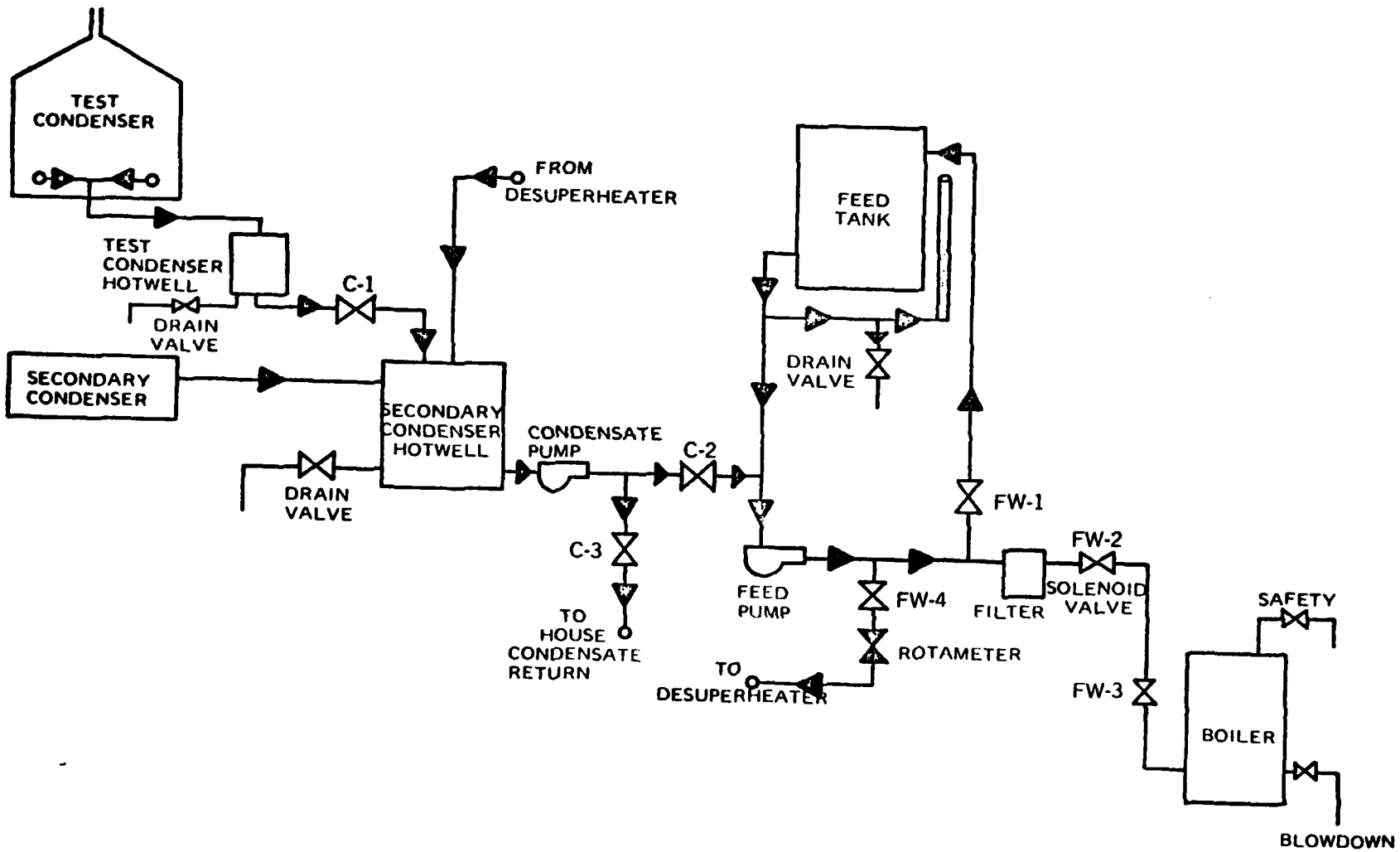

Fig. 7. Schematic Diagram of Condensate and Feedwater System

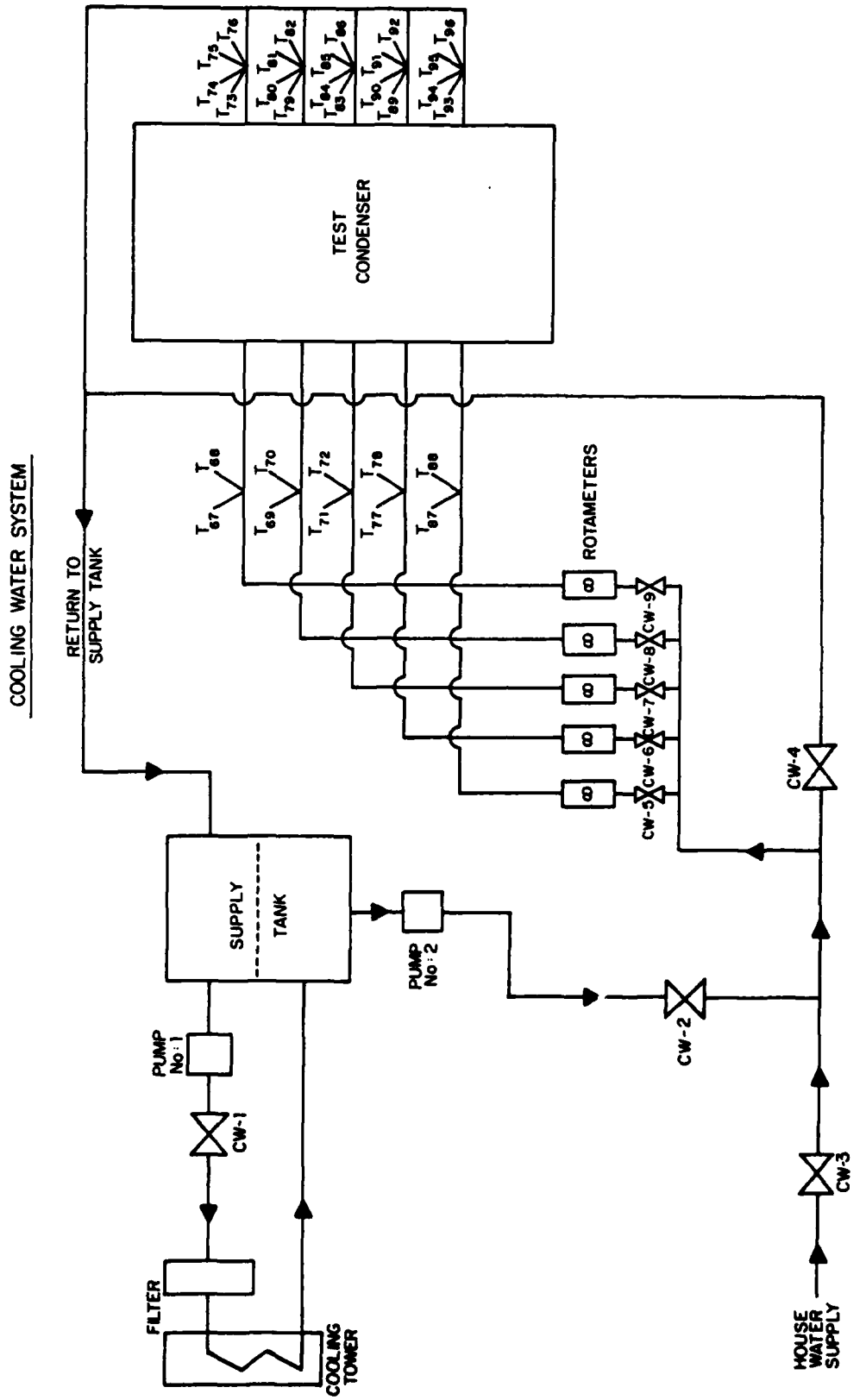

Fig. 8 Schematic Diagram of Cooling Water System.

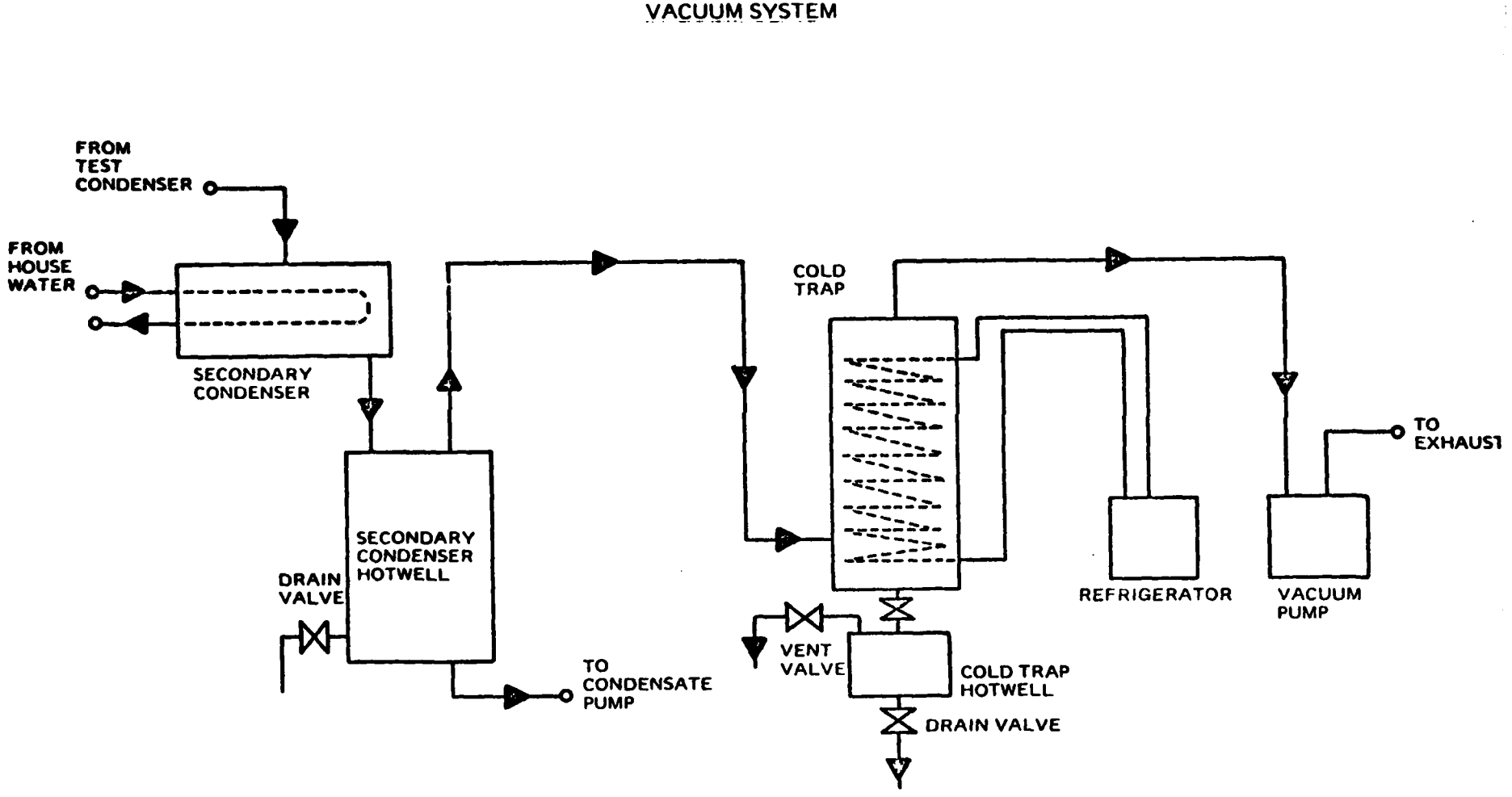

Fig. 9. Schematic Diagram of Vacuum System

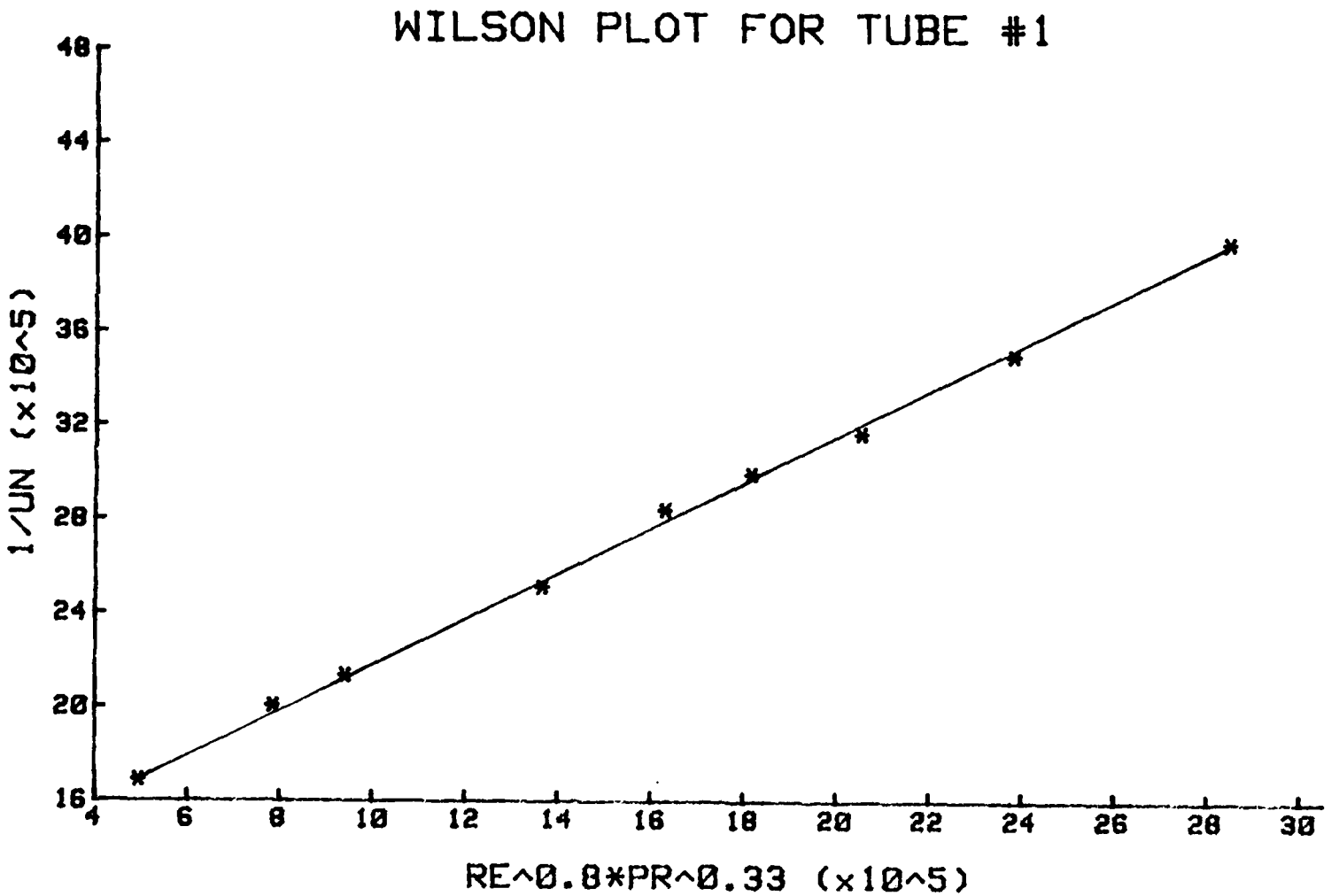

Fig. 10. Wilson Plot for Tube Number 1

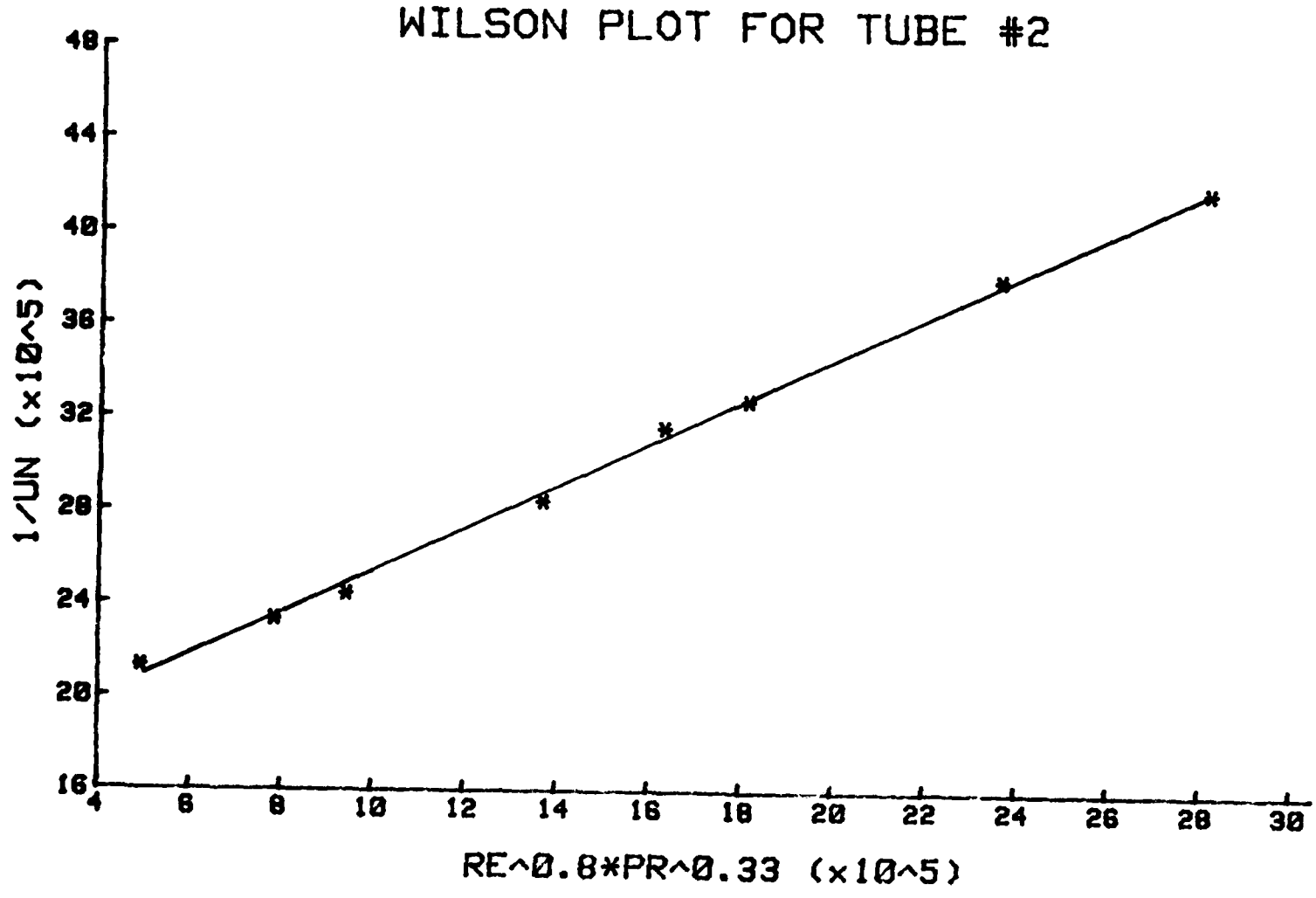

Fig. 11. Wilson Plot for Tube Number 2

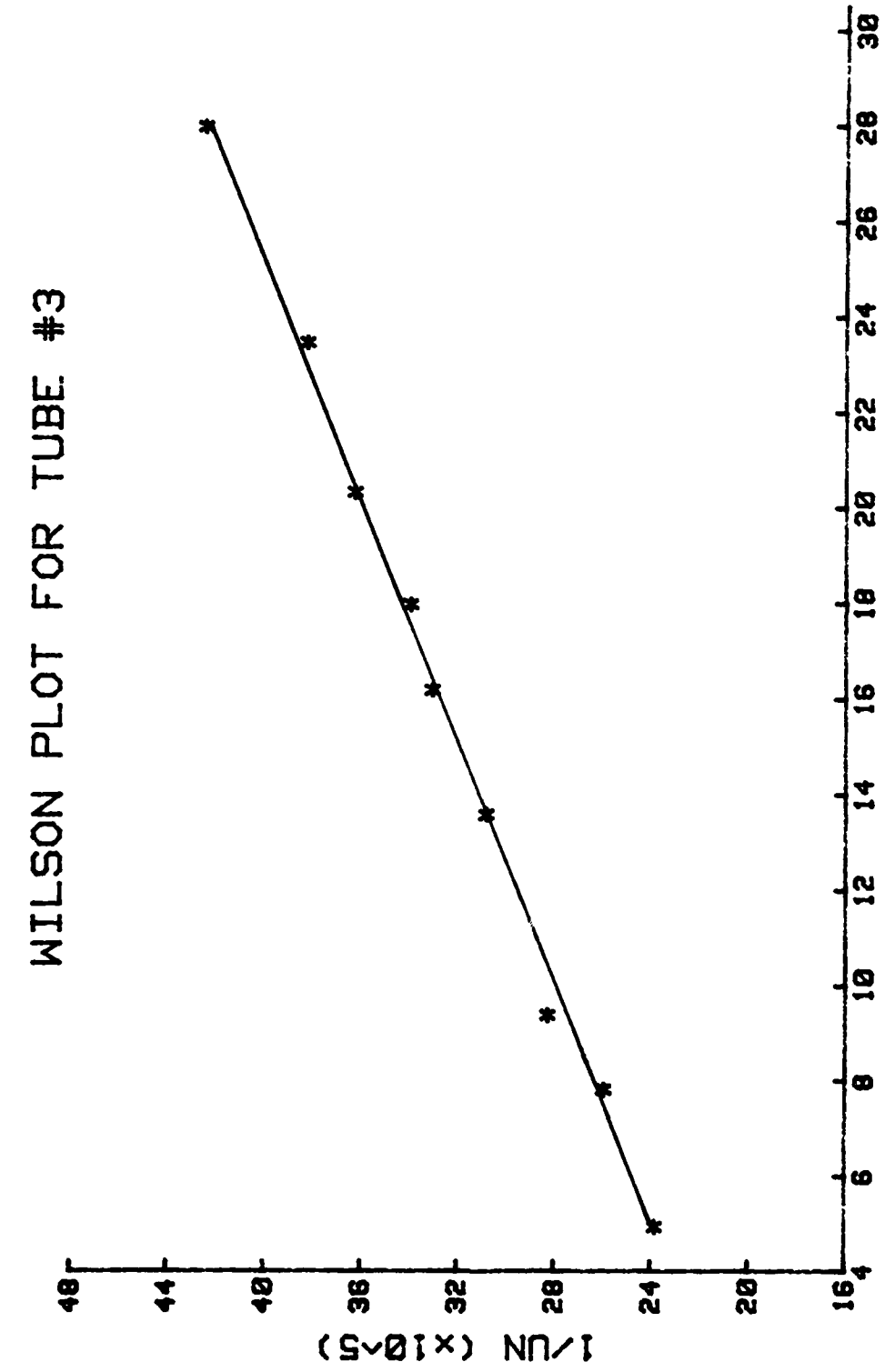

Fig. 12. Wilson Plot for Tube Number 3

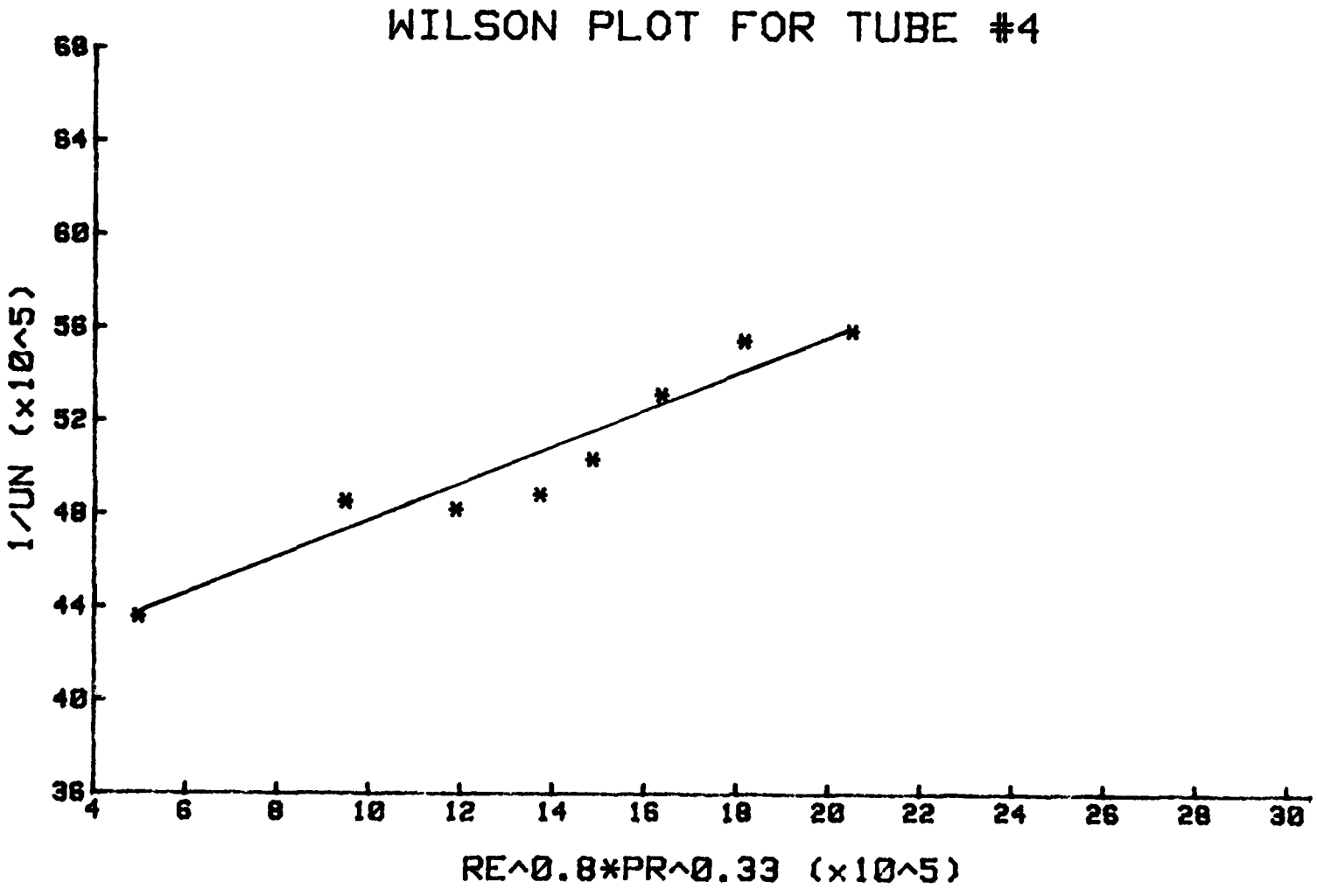

Fig. 13. Wilson Plot for Tube Number 4

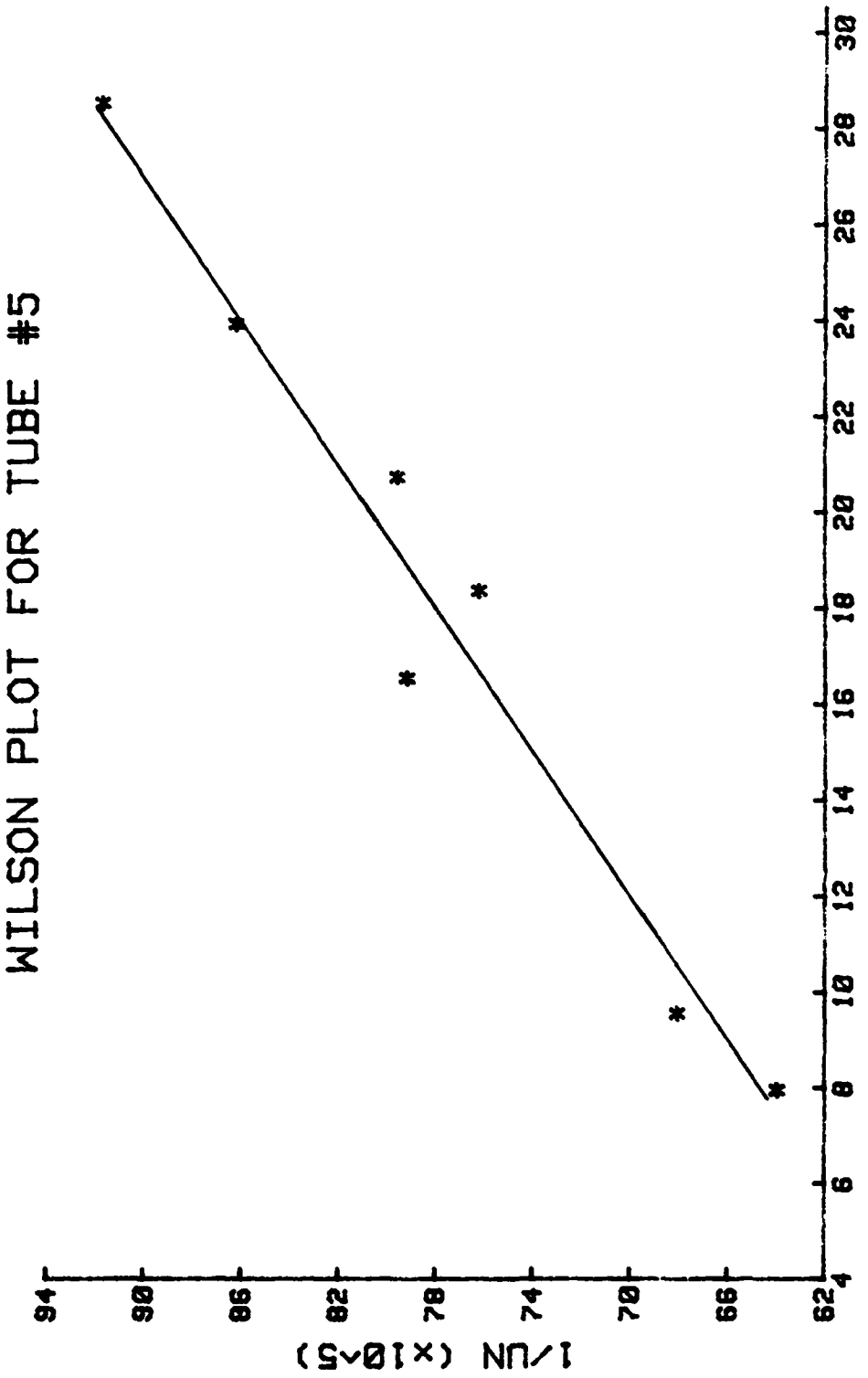

Fig. 14. Wilson Plot for Tube Number 5

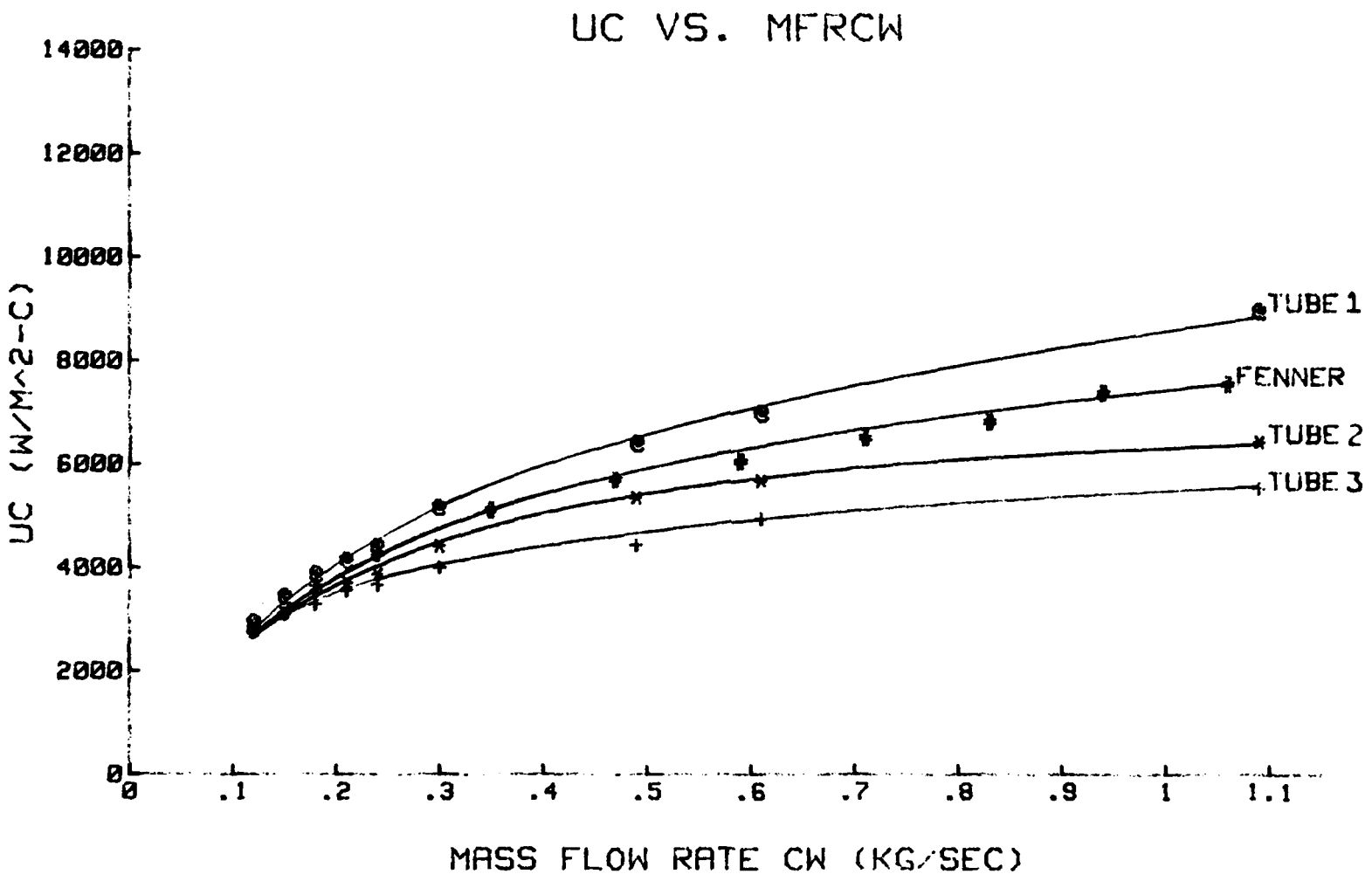

Fig. 15. Comparison of Corrected Overall Heat Transfer Coefficient for Tubes 1, 2, 3 with Fenner [5]

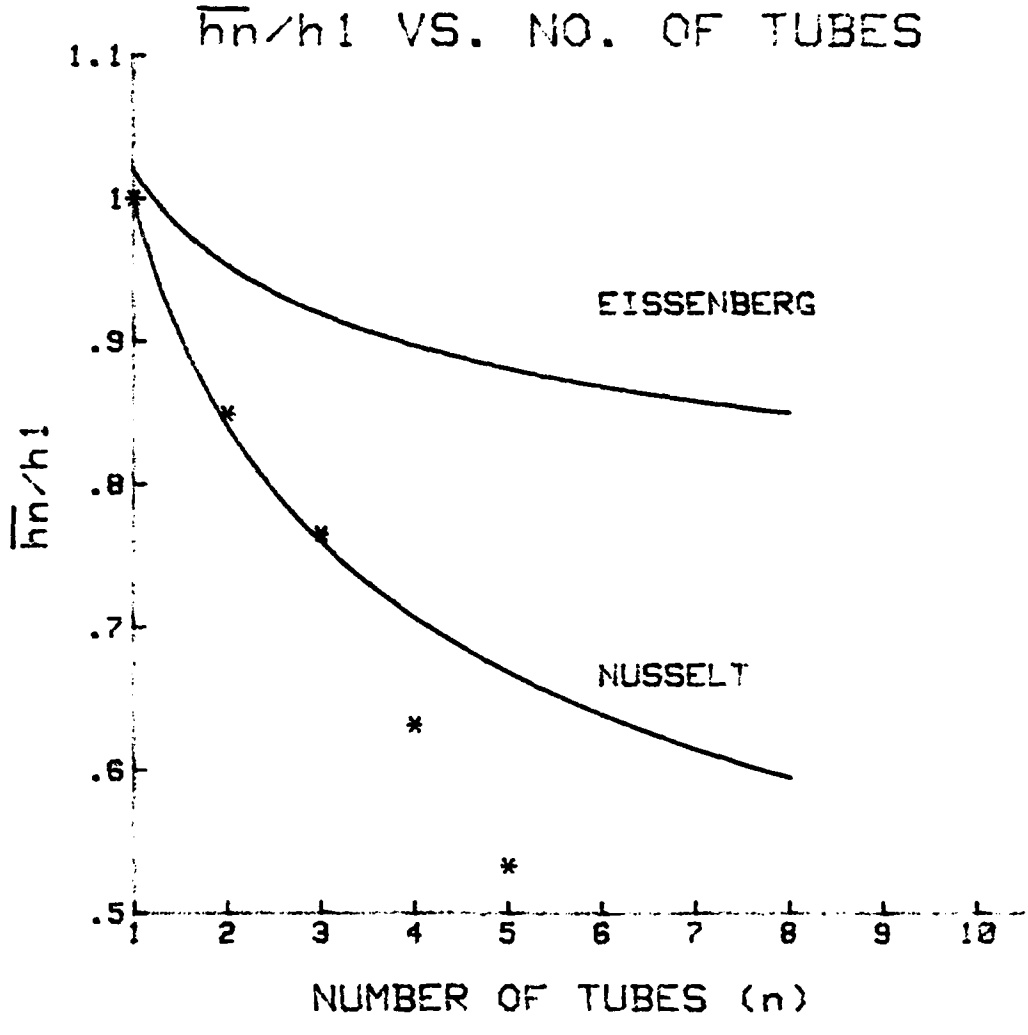

Fig. 16. Average Outside Heat Transfer Coefficient Ratio Versus No. of Tubes

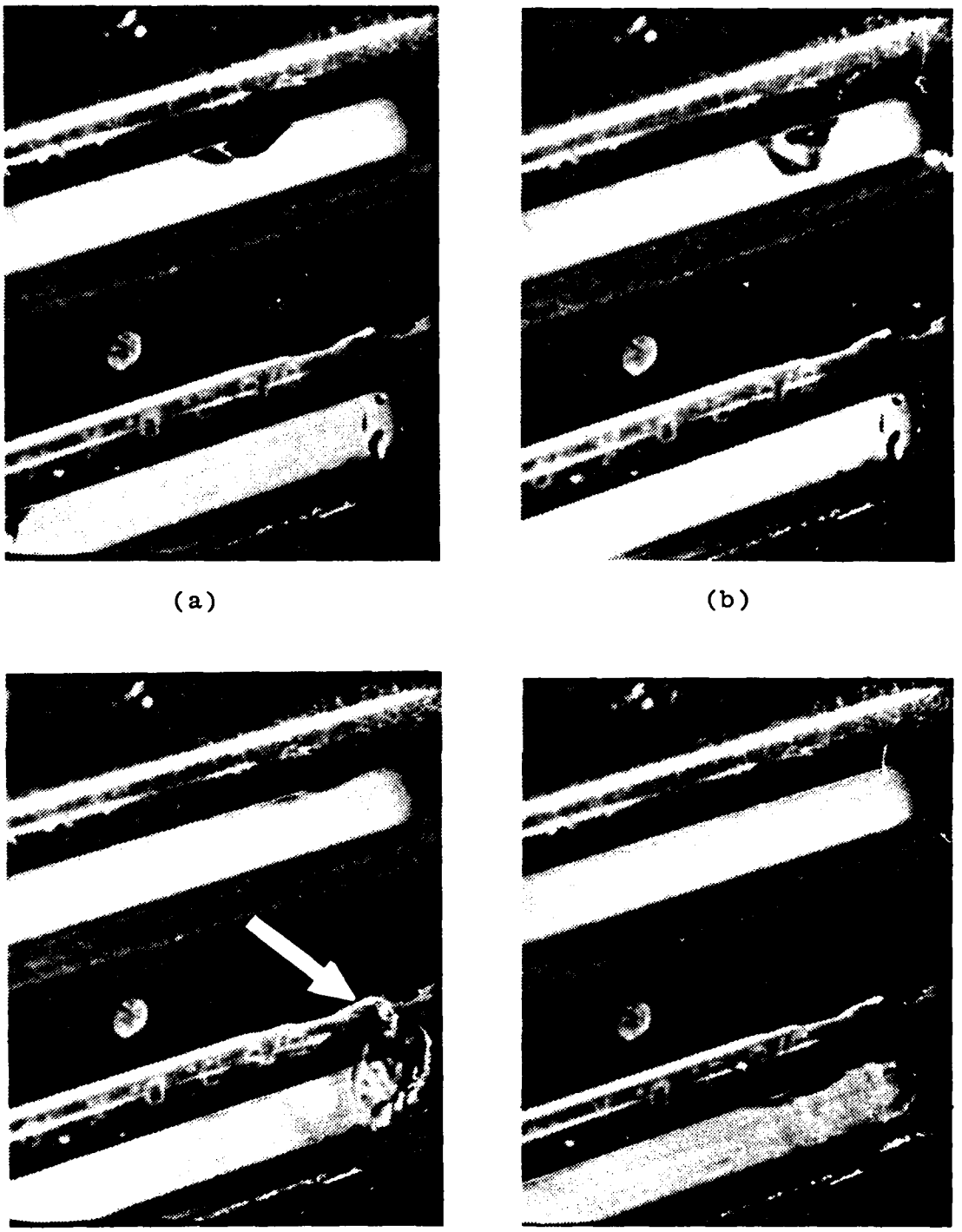

Fig. 17. Sequence of Photographs Showing Side Drainage of Droplet

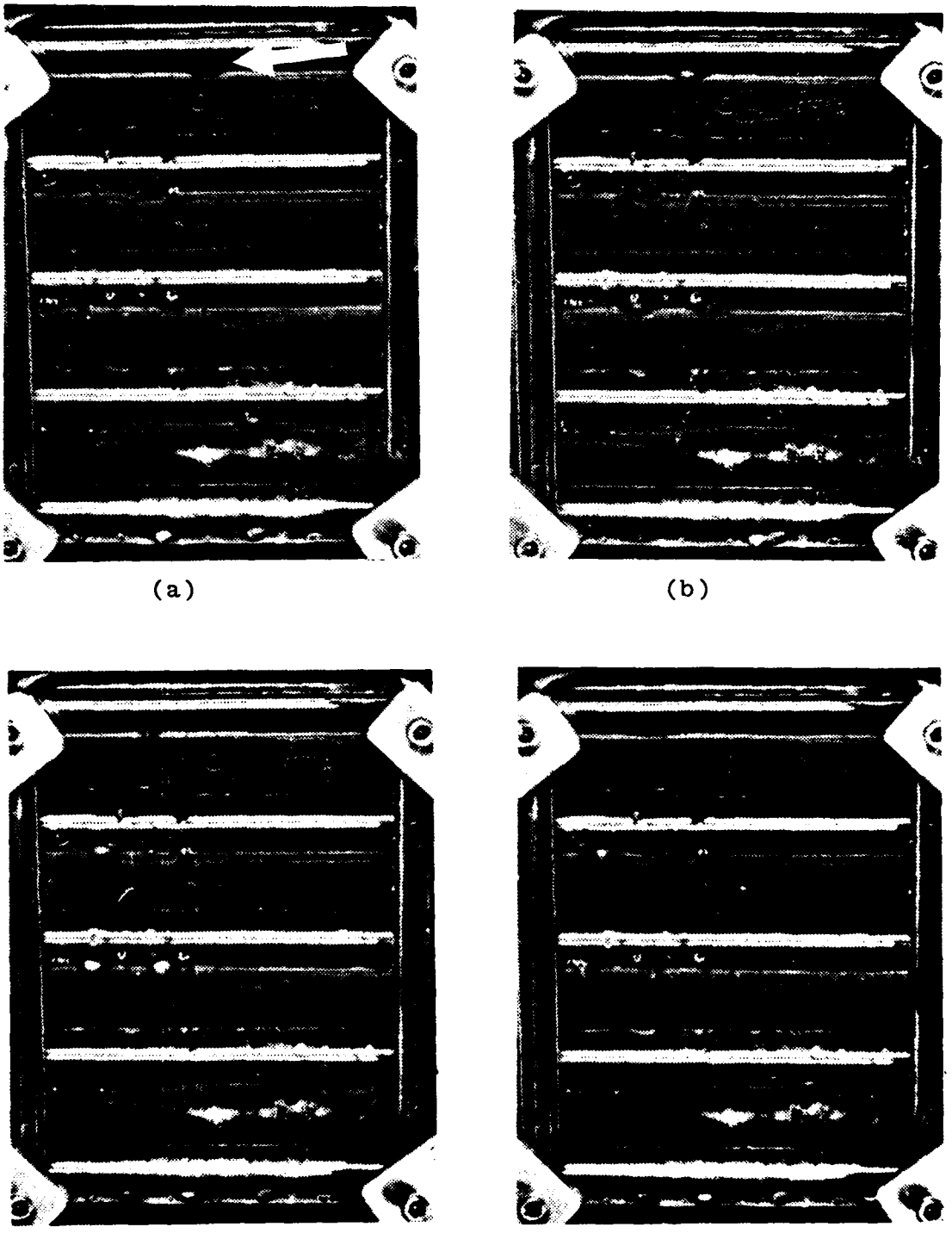

Fig. 18. Sequence of Photographs Showing Droplet Migration

APPENDIX A

Sample Calculations

The following is an example of how the data reduction program progresses to the results. Tube number 1 at 25% flow was selected for this analysis. This same tube and flow rate was used for the error analysis in Appendix B.

Input Parameters

Outside Diameter (D_o)	0.015875m
Inside Diameter (D_i)	0.0141m
Tube Length (L)	0.9144m
Outside Nominal Surface Area (A_n)	$0.0456 m^2$
Wall Resistance (Rw)	$5.72 \times 10^{-5} m^2$ - K/W
Cooling Water Temperature Inlet (T_{ci})	24.1 C
Cooling Water Temperature Outlet (T_{co})	29.4 C
Average Cooling Water Temperature (T_{bc}, T_{bk})	26.75 C, 299.9 K
Steam Vapor Temperature (T_{sv})	64.0 C
Gallons Per Minute of Cooling Water (GPM)	4.80 GPM

Section 1. Water Properties

$$\mu(MHUW) = (4.134 \times 10^{-4}) \exp\{[(0.008291758)(299.9) + (2644.2189)/(299.9)] - 10.59252566\}$$

$$\mu = 8.418 \times 10^{-4} \text{ kg/m-sec}$$

- -

$$k(Kw) = 0.5565919 + (0.002174417)(26.75) - (0.70127 \times 10^{-5}) \cdot (26.75)^2 - (2.0914 \times 10^{-10})(26.75)^3$$

$$k = .6097355 \text{ W/m - C}$$

$$\rho(RHO) = 100.444434 - (0.12673368)(26.76) - (0.0023913147)(26.75)^2$$

$$\rho = 999.343 \text{ kg/m}^3$$

$$C_p(CP) = 4.2377955 - (0.0018553514)(26.75) + (1.3948314 \times 10^{-5})(26.75)^2$$

$$C_p = 4.198 \text{ kJ/kg - C}$$

$\dot{m}$(MFRCW) = LPM x RHO x 1.67 x 10^{-5}, where LPM = GMP x 3.78533

= 18.169584 x 999.343 x 1.67 x 10^{-5}

$\dot{m}$ = 0.30323 kg/sec

Prandtl Number (Pr)

$Pr = \mu C_p/k = (8.418 \times 10^{-4} \times 4.198 \times 10^{3})/.6097355$

Pr = 5.796

Section 2. Data Reduction

1. Cooling Water Velocity (C_{wv}) = $4\dot{m}/\rho\pi D_i^2$

$C_{wv} = (4)(.30323)/(999.343)(\pi)(.0141)^2$

$C_{wv} = 1.943 m/sec$

---

2. Mass Flow Rate Per Unit Area (G)

$G = 4\dot{m}/\pi D_i^2 = (\rho)(C_{wv})$

$G = (999.343)(1.943)$

$G = 1941.72\ kg/m^2 - sec$

---

3. Reynolds Number (Re)

$Re = D_i\ G/\mu = (.0141)(1941.72)/8.418 \times 10^{-4}$

$Re = 32,523.46$

---

4. Determination of Overall Heat Transfer Coefficient (U_n)

$$U_n = \frac{\dot{m}\ C_p}{A_n}\ \ell n\ \left(\frac{T_{sv} - T_{ci}}{T_{sv} - T_{co}}\right)$$

$$= \frac{(.30323)(4.198 \times 10^3)}{.0456}\ \ell n\ \left(\frac{64 - 24.1}{64 - 29.4}\right)$$

$U_n = 3978.63\ W/m^2 - C$

---

5. Determination of Corrected Overall Heat Transfer Coefficient (U_c)

$$U_c = \frac{1}{\frac{1}{U_n} - R_w} = \frac{1}{\frac{1}{3978.63} - 5.72 \times 10^{-5}}$$

$$U_c = 5150.85 \text{ W/m}^2 - \text{C}$$

---

6. Determination of Wilson Plot Parameters

(a) Ordinate

$$Y = \frac{1}{U_n} = \frac{1}{3978.63}$$

$$Y = 25.13 \times 10^{-5} \text{ m}^2 \text{ C/W}$$

(b) Abscissa

$$X = \frac{1}{Re^{0.8} Pr^{1/3}} = \frac{1}{(32,523.46)^{0.8} (5.796)^{1/3}}$$

$$X = 13.67 \times 10^{-5}$$

---

7. Determination of Constant

$$C = \frac{D_o}{Mk}, \quad \text{where M = slope returned by linear regression subroutine}$$

$$M = .9735$$

$$C = \frac{0.015875}{(.9735)(.6097355)} = .027$$

---

8. Determination of Inside Heat Transfer Coefficient (h_i)

$$Nu = \frac{h_i D_i}{k} = 0.036\ Re^{0.8}\ Pr^{1/3}\ (L/Do)^{-0.054}$$

where

$$L/D = \frac{.9144}{.015875} = 57.6$$

$$h_i = \frac{k}{D_i} .029\ Re^{0.8}\ Pr^{1/3}$$

$$h_i = .029(32,523.46)^{0.8}\ (5.796)^{1/3}\ \frac{(.6097355)}{(.0141)}$$

$$h_i = 9171.78\ W/m^2 - C$$

- -

9. Determination of Outside Heat Transfer Coefficient

$$h_o = \frac{1}{\frac{1}{Un} - Rw - \frac{D_o}{D_i\ h_i}} = \frac{1}{\frac{1}{3978.63} - 5.72 \times 10^{-5} - \frac{(.015875)}{(.0141)(9171.78)}}$$

$$h_o = 14,008\ W/m^2 - C$$

APPENDIX B

Error Analysis

The basic equations used in this section are reproduced from Reilly [4]. The general form of the Kline and McClintock [13] "second order" equation is used to compute the probable error in the results. For some resultant, R, which is a function of primary variables X_1, X_2, ..., X_n, the probable error in R, δR is given by:

$$\delta R = \left[\left(\frac{\delta R}{\delta X_1}\,\delta X_1\right)^2 + \left(\frac{\delta R}{\delta X_2}\,\delta X_2\right)^2 + \ldots + \left(\frac{\delta R}{\delta X_n}\,\delta X_n\right)^2\right]^{1/2} \tag{B-1}$$

where δX_1, δX_2., ..., δX_n is the probable error in each of the measured variables.

1. Uncertainty in Overall Heat Transfer Coefficient, U_n

$$\frac{\delta U_n}{U_n} = \left[\left(\frac{\delta A_n}{A_n}\right)^2 + \left(\frac{\delta C_p}{C_p}\right)^2 + \left(\frac{\delta \dot{m}}{\dot{m}}\right)^2 + \left(\frac{\delta T_{sv}(T_{ci} - T_{co})}{(T_{sv}-T_{ci})(T_{sv}-T_{co})\,\ell n\,\frac{T_{sv}-T_{ci}}{T_{sv}-T_{co}}}\right)^2 + \left(\frac{\delta T_{ci}}{(T_{sv}-T_{ci})\,\ell n\,\frac{T_{sv}-T_{ci}}{T_{sv}-T_{co}}}\right)^2 + \left(\frac{\delta T_{co}}{(T_{sv}-T_{co})\,\ell n\,\frac{T_{sv}-T_{ci}}{T_{sv}-T_{co}}}\right)^2\right]^{1/2}$$

The following values are assigned to the variables:

$\delta A_n = \pm 0.0001\ m^2$

$\delta C_p = \pm .0042\ KJ/Kg - C$

$$\delta\dot{m} = \pm .01 \text{ kg/sec}$$

$$\delta T_{sv} = \pm .5 \text{ C}$$

$$\delta T_{ci} = \pm .1 \text{ C}$$

$$\delta T_{co} = \pm .1 \text{ C}$$

For Tube #1 at 25% Flow:

$$\frac{\delta U_n}{U_n} = \left[\left(\frac{.0001}{.0456}\right)^2 + \left(\frac{.0042}{4.198}\right)^2 + \left(\frac{.01}{.30323}\right)^2 + \left(\frac{(.5)(-5.3)}{(39.9)(34.6)\,\ell n\ 1.153}\right)^2 + \left(\frac{.1}{(39.9)\,\ell n\ 1.153}\right)^2 + \left(\frac{.1}{34.6\ \ell n\ 1.153}\right)^2\right]^{1/2}$$

$$\frac{\delta U_n}{U_n} = .044$$

U_n Tube #1 - 25% = 3978 ± 175 W/m^2 - C

2. Uncertainty in Inside Heat Transfer Coefficient (hi)

The probable error in the inside heat transfer coefficient is given by:

$$\frac{\delta h_i}{h_i} = \left[\left(\frac{\delta k}{k}\right)^2 + \left(\frac{\delta D_i}{Di}\right)^2 + \left(\frac{0.8\delta Re}{Re}\right)^2 + \left(\frac{0.333\delta Pr}{Pr}\right)^2 + \left(\frac{\delta C}{C}\right)^2\right]^{1/2}$$

where

$$\delta k = \pm 0.001 \text{ W/m - C}$$

$$\delta D_i = \pm 0.001 \text{ m}$$

$$\delta Pr = \pm 0.10$$

$$\delta C = \pm 0.001$$

$$\frac{\delta Re}{Re} = [(\frac{\delta G}{G})^2 + (\frac{\delta \mu}{\mu})^2 + (\frac{\delta D_i}{D_i})^2]^{1/2} = [(.01)^2 + (\frac{.10}{8.418})^2 + (\frac{.001}{.0141})^2]^{1/2}$$

$$= .073$$

$$\frac{\delta h_i}{h_i} = [(\frac{.001}{.6097})^2 + (\frac{.001}{.0141})^2 + (.8 \quad .073)^2 + (\frac{.333 \quad .1}{5.796}) + (\frac{.001}{.029})^2]^{1/2}$$

$$= .098$$

h_i, Tube #1 25% = 9171 ± 901 W/m^2 - C

3. Uncertainty in the Outside Heat Transfer Coefficient (h_o)

The probable error in the outside heat transfer coefficient is given by:

$$\frac{\delta h_o}{h_o} = \{[\frac{\delta U_n}{U_n^2 (\frac{1}{U_n} - Rw - \frac{D_o}{D_i h_i})}]^2 + [\frac{\delta Rw}{(\frac{1}{U_n} - Rw - \frac{D_o}{D_i h_i})}]^2 + [\frac{(\frac{D_o}{D_i h_i})(\frac{\delta h_i}{h_i})}{\frac{1}{U_n} - Rw - \frac{D_o}{D_i h_i}}]^2\}^{1/2}$$

where

$$\frac{\delta U_n}{U_n} = .044$$

$$\delta Rw = 2.86 \times 10^{-6}\ m^2 - C/W$$

$$\frac{\delta h_i}{h_i} = .098$$

$$\frac{1}{U_n} - Rw - \frac{Do}{Di\ hi} = 7.14 \times 10^{-5}\ m^2 - C/W$$

$$\frac{\delta ho}{h_o} = \left\{\left[\frac{.044}{(3978.63)(7.14 \times 10^{-4})}\right]^2 + \left[\frac{2.86 \times 10^{-6}}{7.14 \times 10^{-5}}\right]^2 + \left[\frac{(1.2276 \times 10^{-4})(.098)}{7.14 \times 10^{-5}}\right]^2\right\}^{1/2}$$

$$\frac{\delta h_o}{h_o} = .174$$

$$h_o = 14{,}008 \pm 2435\ W/m^2 - C$$

BIBLIOGRAPHY

1. Search, H. T., A Feasibility Study of Heat Transfer Improvement in Marine Steam Condensers, MSME, Naval Postgraduate School, Monterey, California, December 1977.

2. Beck, A. C., A Test Facility to Measure Heat Transfer Performance of Advanced Condenser Tubes, MSME, Naval Postgraduate School, Monterey, California, January 1977.

3. Pence, D. T., An Experimental Study of Steam Condensation on a Single Horizontal Tube, MSME, Naval Postgraduate School, Monterey, California, March 1978.

4. Reilly, D. J., An Experimental Investigation of Enhanced Heat Transfer on Horizontal Condenser Tubes, MSME, Naval Postgraduate School, Monterey, California, March 1978.

5. Fenner, J. H., An Experimental Comparison of Enhanced Heat Transfer Condenser Tubing, MSME, Naval Postgraduate School, Monterey, California, September 1978.

6. Manvel, J., An Experimental Study of Dropwise Condensation on Horizontal Condenser Tubes, MSME, Naval Postgraduate School, Monterey, California, June 1979.

7. Ciftci, H., An Experimental Study of Filmwise Condensation on Horizontal Enhanced Condenser Tubing, MSME, Naval Postgraduate School, Monterey, California, December 1979.

8. Boushanskii, V. M. and Paleev, I. I., Convective Heat Transfer in Two Phase and One Phase Flows, Russia, 1969.

9. Skklover and Buevich, "The Mechanism of Film Flow with Steam Condensation in Horizontal Bundle of Tubes," Techernergetika, p. 46-49, 1978.

10. Eissenberg, D. M., An Investigation of the Variables Affecting Steam Condensation on the Outside of a Horizontal Tube Bundle, Ph.D. Thesis, University of Tennessee, Knoxville, December 1972.

11. Fujii, T., "Vapor Shear and Condensate Inundation," Research Institute of Industrial Science, Kijushu University, Fukuoka, Japan, 1979.

12. Croix, J. M., and Liegeois, A., "Condensation Dans in Faiscean Tubulaire Horizontal," Department of Transfer and Conversion of Energy Service of Thermic Transfers, France, 1978.

13. Kline, S. J. and McClintock, F. A., Describing Uncertainties in Single Sample Experiments, Mech. Engin., Vol. 74, pp. 3-8, January 1953.

INITIAL DISTRIBUTION LIST

		No. Copies
1.	Defense Technical Information Center Cameron Station Alexandria, Virginia 22314	2
2.	Library, Code 0142 Naval Postgraduate School Monterey, California 93940	2
3.	Department Chairman, Code 69 Department of Mechanical Engineering Naval Postgraduate School Monterey, California 93940	2
4.	Professor P. J. Marto, Code 69Mk Department of Mechanical Engineering Naval Postgraduate School Monterey, California 93940	5
5.	LCDR Donald E. Eshleman, USN 835 Chew Street Allentown, Pennsylvania 18102	2
6.	Mr. Charles Miller Naval Sea Systems Command (0331) 2221 Jefferson Davis Highway, CP#6 Arlington, Virginia 20360	1
7.	Mr. Wayne L. Adamson Naval Ship Research and Development Center (2761) Annapolis, Maryland 21402	1
8.	Dr. David Eissenberg Oakridge National Laboratory Post Office Box Y Oak Ridge, Tennessee 37830	1
9.	Mr. Kurt Bredehorst NAVSEC 6147D Department of the Navy Hyattsville, Maryland 02782	1